Review

Hedieh Malekzad, Parham Sahandi Zangabad, Hamed Mirshekari, Mahdi Karimi* and Michael R. Hamblin*

Noble metal nanoparticles in biosensors: recent studies and applications

DOI 10.1515/ntrev-2016-0014
Received March 23, 2016; accepted September 16, 2016; previously published online December 21, 2016

Abstract: The aim of this review is to cover advances in noble metal nanoparticle (MNP)-based biosensors and to outline the principles and main functions of MNPs in different classes of biosensors according to the transduction methods employed. The important biorecognition elements are enzymes, antibodies, aptamers, DNA sequences, and whole cells. The main readouts are electrochemical (amperometric and voltametric), optical (surface plasmon resonance, colorimetric, chemiluminescence, photoelectrochemical, etc.) and piezoelectric. MNPs have received attention for applications in biosensing due to their fascinating properties. These properties include a large surface area that enhances biorecognizers and receptor immobilization, good ability for reaction catalysis and electron transfer, and good biocompatibility. MNPs can be used alone and in combination with other classes of nanostructures. MNP-based sensors can lead to significant signal amplification, higher sensitivity, and great improvements in the detection and quantification of biomolecules and different ions. Some recent examples of biomolecular sensors using MNPs are given, and the effects of structure, shape, and other physical properties of noble MNPs and nanohybrids in biosensor performance are discussed.

Keywords: biomolecule detection; colorometric; electrochemical; metal nanostructures; nanobiosensor; optical; piezoelectric.

***Corresponding authors: Mahdi Karimi,** Department of Medical Nanotechnology, Faculty of Advanced Technologies in Medicine, Iran University of Medical Sciences, Hemmat Exp. Way, P.O. Box 14665-354, Tehran, Iran, e-mail: m_karimy2006@yahoo.com, karimi.m@iums.ac.ir; and **Michael R. Hamblin,** Wellman Center for Photomedicine, Massachusetts General Hospital, Boston, MA 02114, USA; Department of Dermatology, Harvard Medical School, Boston, MA 02115, USA; and Division of Health Sciences and Technology, Harvard-MIT, Cambridge, MA 02139, USA, e-mail: hamblin@helix.mgh.harvard.edu
Hedieh Malekzad: Faculty of Chemistry, Kharazmi University, South Mofatteh Ave, P.O. Box 15719-14911, Tehran, Iran; and Advanced Nanobiotechnology and Nanomedicine Research Group (ANNRG), Iran University of Medical Sciences, Tehran, Iran
Parham Sahandi Zangabad: Research Center for Pharmaceutical Nanotechnology (RCPN), Tabriz University of Medical Science (TUOMS), Tabriz, Iran; Advanced Nanobiotechnology and Nanomedicine Research Group (ANNRG), Iran University of Medical Sciences, Tehran, Iran; and Department of Materials Science and Engineering, Sharif University of Technology, P.O. Box 11365-9466, 14588 Tehran, Iran
Hamed Mirshekari: Advanced Nanobiotechnology and Nanomedicine Research Group (ANNRG), Iran University of Medical Sciences, Tehran, Iran

Highlights

- Recent developments in noble metal nanoparticle-based biosensors are reviewed.
- The main roles of metal nanoparticles are immobilizing bioreceptors, mediating electron transfer, catalyzing bioreactions, amplifying mass change, and enhancing refractive index changes.
- Electrochemical nanobiosensors can be categorized into five classes: enzymatic, nonenzymatic, aptamer-based, immunoassay-based, and DNA-based biosensors.
- Several anisotropic nanoparticles have been used in surface plasmon resonance applications offering higher sensitivity toward refractive index changes.

1 Introduction

In recent decades, nanotechnology, for its world-leading area role, has brought out miscellaneous innovative applications to be employed in nanomedicine and nanobiotechnology such as drug delivery systems, biosensing and biodetection, finding new therapies for formidable diseases such as cancers, etc. [1–14].

The increasing demand for sensing a broad range of molecules at low concentrations with high specificity has motivated the development of sophisticated devices that

incorporate nanoscale materials, biological elements, and advanced materials, which are collectively called nanobiosensors. Many microorganisms, viruses, bacteria, and pathogens have similar dimensions to those of nanostructures; therefore, the detection specificity is highly increased by utilizing chemically inert and biocompatible nanomaterials for biomedical approaches. Various toxic substances in food and environmental pollutants have also been detected and measured using nanomaterial-based biosensors [15–19].

The main functional components of conventional biosensors include a biological recognition receptor, such as an antibody, enzyme, nucleic acid, and whole cell; a transducer to convert the biological binding event to a detectable signal (electrochemical, optical, etc.); and a signal display or readout that indicates both the presence and concentration of the analyte molecule [20]. According to the biorecognition mechanism, biosensors can be classified into two main categories comprising biocatalytic- and bioaffinity-based biosensors. In the biocatalytic system, the bioreceptor (enzyme, whole cell, tissue, etc.) recognizes the analyte and catalyzes a reaction leading to consumption of the analyte, while in the bioaffinity system, the bioreceptor (e.g. antibody or aptamer) specifically binds to the analyte and an equilibrium is usually reached [21]. In Table 1, common types of biosensors according to different transduction pathways are listed and the related typical biological recognizing elements which are used for each type is defined.

In nanobiosensors, nanostructures are often incorporated into the biosensor by attachment to the suitably modified platforms. Metal nanoparticles (MNPs) have many advantageous properties that make them useful in the transducer component of biosensors. Many metal and metal-organic nanoparticles (NPs) have been used in nanobiosensors. Noble metals such as gold, silver, and platinum NPs have been the most popular and have been extensively studied. While these noble metals are chemically inert in their macroscale form, they display unique physiochemical features at the nanoscale [22].

Herein, we will solely focus on nanobiosensors with noble MNP component and the advantages it offers in terms of sensitivity and selectivity. More comprehensive considerations on biosensors, recent advances, and potential future applications are available elsewhere [23–26].

In this review, the functions of various noble MNPs with various anisotropies (spherical, nanohole, triangular, etc.) and in distinct forms of nanowire arrays, nanotube arrays, bimetallic alloys, core-shell structures, etc., will be discussed. Each form of these MNPs exhibits interesting surface and interface features, which significantly improves the biocompatibility and transduction of the biosensor in comparison to the same process in the absence of these MNPs.

The roles of these MNPs can be defined according to the physical or electrochemical changes that occur after binding the biomolecular analyte and the immobilized receptor-target on the surface of the MNPs. Based upon their specific properties, NPs can act as immobilizing platforms [27–31], accelerate electron transfer [32, 33], catalyze the reaction of chemiluminecents with their substrates [34–37], amplify changes in mass [38, 39] and enhance refractive index (RI) changes [40, 41]. For instance, in addition to immobilizing the bioreceptors, MNPs can act

Table 1: Biosensor types, relevant transduction pathway, common techniques employed for each transduction pathways, and prevalent biorecognizing agents for each type.

Biosensor according to transducer type	Type of change detected	Biological recognizer element	Common techniques
Electrochemical	Redox reaction/electrical conductivity as a result of change in ion concentration	Enzyme Antibody Aptamer DNA Microbial cells	Amperometric Potentiometric Conductometric
Piezoelectric	Resonant frequency of crystals due to change in mass	Antibody Nucleic acid (DNA, RNA)	Crystal resonance frequency Surface transverse wave Surface acoustic wave
Optical (optoelectric) biosensors	Fluorescence/absorbance and other optical properties	Enzyme Antibody Nucleic acids Aptamer Microbial cells	SPR Fiber optics Light addressable potentiometric Colorimetric
Calorimetric biosensors	Temperature changes	Enzymes	Thermistors

as "electron wires" in electrochemical biosensors, which allow electrons produced in bioreactions to be transported to sensing electrodes or convert other physiochemical changes to measurable signals that are proportional to the analyte concentration [32]. A general schematic presenting some applications of noble MNPs in conjugation with biological recognition elements and a linear pathway describing biosensing process of a specific analyte, from recognition of the analyte by receptor, transduction of the change resulted from binding event, its conversion to measurable signal, signal processing, and finally signal display is demonstrated in Figure 1.

2 The functions of MNPs in various biosensor types

2.1 Electrochemical nanobiosensors

The use of electrochemical transduction in nanobiosensors usually relies on amperometry or voltammetry techniques. Voltammetric measurements are made by applying a range of electric potentials and recording the occurring current (that results from a redox reaction) to determine the peak value. On the other hand, amperometry is performed by fixing the potential at a suitable value (which is characteristic of the analyte) and recording the current changes versus time [33]. MNPs are used as labels to improve the sensitivity and enhance analytical signal detection in electrochemical biosensors. Ding et al. [42] have defined four approaches for using MNPs as labels in electrochemical biosensors: (1) using MNPs to increase the loading of electroactive species; (2) MNPs that function as ultra microelectrode arrays for the electrolysis of large amounts of substrate; (3) to catalyze the electrochemical deposition of detectable species; and (4) to mediate the deposition of electrocatalysts. There are some drawbacks associated with using noble MNPs as labels in electrochemical biosensors. One major limitation for the first approach is the need for a subsequent step of dissolving labels off the electrode surface by strong oxidizing reagent, to make them detectable by voltammetric techniques. This step is not cost effective for commercial laboratories with high throughput assays. Other approaches may suffer from a mass transport issue, which is due to the nonspecific adsorption of labels in high concentration and because of incompatibility between the adsorption isotherm plot of the analyte and the calibration curve of the biosensor, which occurs due to the shift of linear calibration curve toward the lower concentration region compared to the linear region of the adsorption isotherm. In the first approach, the analytical signal is proportional to the extent of coverage of labels on the electrode surface, as well as the surface coverage of the analyte.

2.1.1 Enzymatic electrochemical biosensors

The history of biosensors dates back to 1962, when Clark proposed the first enzymatic glucose sensing device by incorporating the glucose oxidase enzyme (GOD) into an oxygen electrode [43]. Ever since, many efforts have been made to improve the original basic glucose

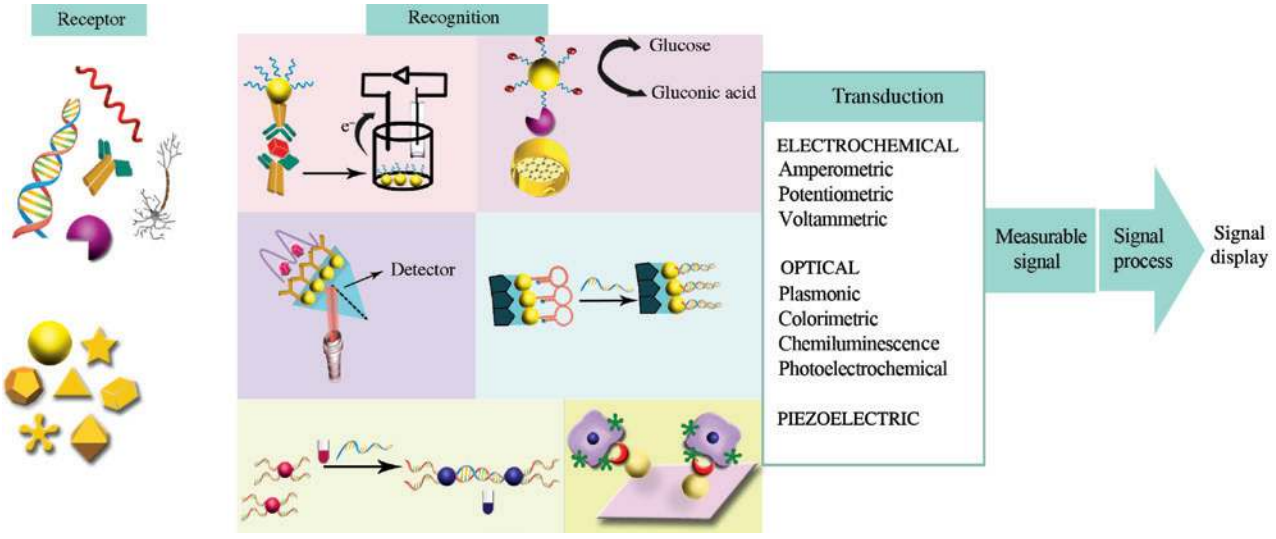

Figure 1: The role of noble MNPs in various types of biosensors.

enzymatic-biosensor and to develop it in order to apply it to other biologically important molecules.

An enzymatic reaction can be coupled with electrochemical detection by two common approaches: mediator-based electron transfer and direct electron transfer. In the first approach, both the analyte (first substrate) and the mediator (second substrate) are transformed (by reduction and oxidation), and eventually, the electrons interact with the electrode surface. In the second approach, the enzyme transforms the substrate into the product and transfers the electrons directly to the electrode [44].

Glucose biosensors, due to their applications in diagnosis and management of diabetes, are of great importance, and novel electrochemical glucose nanobiosensors have been proposed using different modifications that have been applied to electrodes and nanostructures. Nanoscale metallic materials have been employed in amperometric nanobiosensors. In a report published by Cui et al. [45], an amperometric glucose detector based on gold nanowire arrays (AuNWA) with glucose oxidase (GOx) as a bioreceptor, was developed. The electrochemical properties were studied at different scan rates using cyclic voltammetry with a redox system. Amperometric detection of glucose was performed by taking advantage of the oxidation reaction of glucose that produced H_2O_2, which subsequently got transferred to the AuNWA surface, where its oxidation potential gave a current directly proportional to the glucose concentration. The low detection limit reported for glucose in this study was attributed to the high electroactivity of AuNWA (six times larger than a normal gold electrode). In another study, glucose was detected using a modified platinum electrode composed of GO immobilized on platinum NPs (diameter 10–30 nm) deposited on a polyvinylferrocenium perchlorate matrix. The amperometric results showed a signal related to electron transfer from H_2O_2 as a byproduct of the enzymatic reaction. Furthermore, a signal enhancement was also obtained using a voltammetric measurement system with Pt NPs that was due to the electrocatalytic effects of these NPs [27].

A synergistic effect by employing two different kinds of noble MNPs as an electrochemical biosensor was investigated, and they proved an enhancement in electron transfer. It was demonstrated that Pd-Co alloy NPs embedded in carbon nanofibers demonstrated superior analytical ability toward hydrogen peroxide and also nitrite sensing. This synergistic effect was evident in a lower overpotential and considerably higher reduction currents for H_2O_2 and an increased oxidation peak and decreased overpotential in nitrite cyclic voltammograms [46]. In another study [28], Rh NPs and Au NPs were used in the construction of an amperometric glucose biosensor. Rh NP-modified Pt electrode provided a large surface area, with many active sites offering improved electrocatalytic activity. On the other hand, Au NPs, being located in close proximity to the active regions of the enzyme, readily catalyzed the oxidation reaction of peroxide molecules and enhanced the sensitivity of the glucose sensor.

Reduced graphene oxide (RGO) is a highly conductive material and is especially suitable for enzyme-based biosensors because of its biocompatibility [47]. RGO has been used as a conductive platform with large surface area for nanometal stabilization [48]. Despite its advantages, RGO sheets can become aggregated and cause poor dispersion of particles attached to it. To avoid this, some materials like polypyrrole have been used as a modifier to enhance the functionality of the surface and anchor gold NPs (AuNPs) for amperometric glucose sensing [49]. A novel RGO-modified glucose sensor was developed using a Pd-Pt alloy. The study revealed that this electrode had a lower detection limit, greater sensitivity, and better range of linearity compared with each nanometal (Pt and Pt) used individually in the same biosensor [50].

Many hybrid materials and nanocomposite structures consisted of MNPs, combined with particular conductive polymers and a modified electrode, have been designed for electrochemical glucose sensing. One recent example is an amperometric glucose sensor made of poly (diallyldimethylammonium chloride)-capped AuNPs attached to functionalized graphene (G)/multiwalled carbon nanotubes (MWCNTs) forming a nanocomposite [51]. The positively charged AnNPs electrostatically adsorbed to the negatively charged G/MWCNTs, forming a nanocomposite material. Different characterization techniques revealed that the combination was capable of immobilizing more enzyme molecules, leading to fast and direct electron transfer between enzyme redox sites and the electrode.

Silver NPs (AgNPs) are more affordable than AuNPs and have also been used in the construction of nanocomposite-based biosensors. An amperometric nanocomposite biosensor based on TiO_2 nanotube arrays modified with AgNPs exhibited a satisfactory response toward glucose sensing with a high sensitivity of 1151.98 $\mu A\ mM^{-1}\ cm^{-2}$ and a wide linear range of 50–15.5 mM [52].

Core-shell NPs are an interesting class of hybrid platforms, which have been employed to tailor or tune their properties by changing the identity of the nanomaterial or altering the core-to-shell ratio. The functions of the core material like dispersibility, consumption rate, chemical reactivity or thermal stability, etc., can be controlled through using suitable shell coatings. For instance, colloidal carbon was used as a coating on AgNPs to enhance the

biocompatibility of the potentially toxic AgNPs when used for immobilized graphene oxide (GO), while still getting the benefit of direct electron transfer between the redox centers of GO, through the particles and reaching the electrode [53, 54].

Attempts have been made to develop efficient biosensors for biomolecules other than glucose. A hierarchical nanocomposite based on RGO MWCNTs with a unique three-dimensional (3D) structure and Pt NPs with excellent electrocatalytic property was used to construct a sensitive and selective myoglobin-specific biosensor with a low detection limit of 6 pM [55]. Moreover, a novel dopamine amperometric nanobiosensor based on a nanohybrid consisted of ethylenediaminetetraacetic acid (EDTA), GO, and AuNPs was developed and applied to detect dopamine released from living cells [56]. Lactate is another important biomolecule and has been widely investigated through various analytical approaches. Recently, novel nanobiosensors were fabricated based on lactate oxidase and MNP or nanohybrids to monitor lactate levels for medical diagnostic applications [57–59] and assessment of food quality [60].

There have been a few reports of cation and anion sensing electrochemical enzymatic biosensors with incorporation of noble MNPs. Anion sensing amperometric biosensor was developed by Wang et al. [61] for determination of superoxide anion with copper-zinc superoxide dismutase immobilized on AuNP-chitosan-ionic liquid biocomposite film, which demonstrated a low detection limit of 1.7 nM and high sensitivity toward superoxide anion. Phosphate anion levels in waste waters have been monitored for environmental protection purposes through electrochemical enzymatic biosensors in the absence of noble MNPs by incorporation of single or several enzyme systems, i.e. pyruvate oxidase and electrochemically measuring the dissolved oxygen or other alternative enzyme systems such as nucleoside phosphatase and xhantine oxidase, which generate hydrogen peroxide as a result of enzymatic reaction with phosphate anions [62]. Mercury cation, another prominent environmental pollutant, has been measured by poteniometric biosensor with urease enzyme and AuNPs as immobilization platform [16].

2.1.2 Nonenzymatic electrochemical biosensors

Despite their selectivity and efficiency, enzymes suffer from certain drawbacks such as difficulties in immobilization [63]; therefore, many studies have been conducted to develop enzyme-free biosensors utilizing suitable modified electrodes. In a recently published study, an inorganic nanocomposite was proposed for enzyme-free glucose biosensing. The $SrPdO_3$ perovskite/AuNP-modified graphite electrode demonstrated a low detection limit of 10 μM and high specificity toward glucose. The nonenzymatic detection method relied on glucose chemisorption on the electrode surface through a dehydrogenation reaction giving gluconolactone and, finally, conversion of gluconolactone to gluconate after reaction with hydroxide ions in the solution [64]. Glucose biosensors are probably the most widely studied biosensors due to their applications in monitoring blood glucose levels for managing diabetes. In Table 2, some additional recently developed enzyme-free glucose biosensors using noble MNPs in their construction have been listed.

Table 2: Various noble MNP-modified materials that have been used in enzyme-free glucose biosensors.

Material	Medium	Detection potential (V)	Linear range	Limit of detection	Reference
PdCu/GE	N_2 saturated NaOH 0.1 M	−0.4	2–18 mM	20 μM	[65]
AuNPs/GC	H_2SO_4 0.5 M	0.3	0.1–25 mM	0.05 mM	[66]
NiNPs/GNs	NaOH 0.1 M	0.5	5–550 μM	1.85 μM	[67]
PtNPs/TiO_2 NTA	NaOH 0.1 M	−0.5	1–15 mM	0.2 μM	[68]
CuNPs/ZnO NRA	NaOH 0.1 M	0.7	5 μM–1.1 mM	0.3 μM	[40]
RGO-PMS@AuNPs-GOD/GC	PBS 0.1 M	−0.75	0.01–8 mM	2.5 μM	[69]
NiO/PtNPs/ERGO	NaOH 0.05 M	0.6	0.05–5.66 mM	0.2 μM	[70]
Cu@TiC/C	NaOH 0.1 M	0.6	1.0 μM–1.7 mM	0.2 μM	[71]
Pt-CuO/rGO	NaOH 0.1 M	0.6	0.5 μM–12 mM	0.01 μM	[72]
PtNPs/NPG	PBS 0.1 M	0.4	1.0×10^{-7} M to 2.0×10^{-5} M	7.2×10^{-8} M	[73]
CNT/Au	PBS 0.01 M	−0.28	Up to 50 mM	0.1 mM	[74]
Cu/PSi	NaOH 0.1 M	0.55	1–190 and 190–2300 μM dm^{-3}	0.2 μM	[75]
Pt-Pd NWAs and Pt-PdNTAs	PBS 0.1 M	0.2	Up to 10 mM	0.1 mM	[76]

PBS, phosphate-buffered saline.

2.1.3 MNPs in electrochemical immunosensors and aptasensors

In recent years, extensive studies have been conducted to produce biosensors with clinical diagnostic applications. Specifically, many novel electrochemical immunosensors have been developed by incorporating noble MNPs for their good amplification and electrocatalytic properties. In the fabrication of electrochemical immunosensors, noble MNPs can be used to label either antibodies or the antigens in order to amplify the electrochemical response as a read-out of antibody-antigen binding.

While the enzyme-linked immunosorbent assay (ELISA) approach is a popular and precise technique widely applied for immunodetection of antigen molecules in diagnostic applications, immunosensors with MNP amplification can be potentially substituted for conventional ELISA kits, offering same or even better sensitivity, lower detection time, and minimal washing steps [77, 78]. Jeong et al. [79] developed a highly sensitive electrochemical immunosensor for determination of the carcinoembryonic antigen (CEA) cancer biomarker through immobilizing the first antibody and a mediator (thionine, Th) on a AuNP-encapsulated dendrimer (Den/AuNP) and immobilizing the second antibody on MWCNTs, which were in turn conjugated with two enzymes, glucose oxidase (GOx) and horseradish peroxidase (HRP) as electrochemical labels. Cyclic voltammetry and square wave voltammetry techniques were employed to monitor the reduction of hydrogen peroxide by HRP. Results were compared to the classic ELISA method, showing satisfactory comparability of the two approaches and a much better detection limit for the proposed immunosensor (4.4 ± 0.1 pg/ml) (Figure 2).

Aptamers are RNA oligonucleotide sequences that can act as highly selective biorecognition elements through binding to target molecules by forming specific 3D structures. Aptamers can detect small molecules (that antibodies are incapable of recognizing), and their ability for conformational changes before and after binding to their target, their ease of chemical modification, robustness, and economical production are advantageous [80]. Aptamers combined with nanomaterials can provide excellent transduction features in electrochemical nanobiosensors [19, 81] Wang et al. [82] used porous platinum NPs/cadmium ion and copper ion hybrid as a novel electrochemical label attached to antibodies against CEA and alpha fetoprotein (AFP) for use in an immunosensor. The target biomarkers in human serum sample were captured by these labeled antibodies and detected by differentiated pulse voltammetry (DPV).

An important risk factor for Alzheimer's disease, APOE4 phenotype, was detected using an amperometric immunosensor developed by incorporation of fractal gold nanostructures as antibody carriers. Labeling the antibodies against APOE4 with the HRP enzyme, along with the gold nanostructure, offered excellent sensitivity. In this sandwich-type immunoassay, upon adding hydroquinone (HQ) as an enzyme substrate allowing electron transfer along with H_2O_2, the enzyme catalyzed the oxidation of HQ to quinone, and the change in reductive current, which was proportional to APOE4 concentration, was recorded by chrono-amperometry. A detection limit of 0.3 ng/ml was achieved for this immunosensor [83]. The immunosensor exhibited excellent sensitivity for APOE4 even in the presence of other proteins at concentrations 1000 times the concentration of the analyte. A 60% decrease in signal was recorded for the plain Au electrode (Figure 1-b-A) compared to the fractal Au-based immunosensor, indicating the improved signal amplification achieved by the fractal Au nanostructure. The linear relationship between the logarithms of concentration and current responses was used to show reproducibility, to measure standard deviations and detection limits for two types of immunosensors based on fractal and plain gold structures.

Another unique immunosensor for CEA was reported using a combination of Ag and Au NP based on nanogold/mesoporous carbon foam-mediated silver enhancement [84]. The sensor was exposed to KCl solution, and the AgNPs deposited on the immunosensor surface accelerated the electrochemical behavior of anodic stripping voltammetry in the presence of Cl^- ions. This procedure was performed with and without AuNPs, and a considerable increase in signal due to presence of AuNPs was observed. In another recent study, the Au/Ag/Au core/double shell NPs was proposed as a label for secondary antigen for developing an electrochemical sandwich assay with Au@SH-GS as an immunoreaction platform for detection of squamous cell carcinoma antigen. The amperometric sandwich-type immunosensor showed a low detection limit of 0.18 pg/ml and a good linear range of 0.5–40 pg/ml [85]. Chitosan-AuNPs were prepared and used in construction of an electrochemical immunosensor to detect CEA and AFP. The immune colloidal AuNPs loaded with metal ions were used as labels and chitosan-AuNPs as a platform. The signal tags (metal ions) were detected using DPV [86]. In a recent study, Yang et al. [87] proposed an electrochemical sensor for adenosine detection using aptamers based on target-induced strand release. The steps involved in this strategy were as follows: (1) the biotin-labeled adenosine-binding-aptamer/thiol

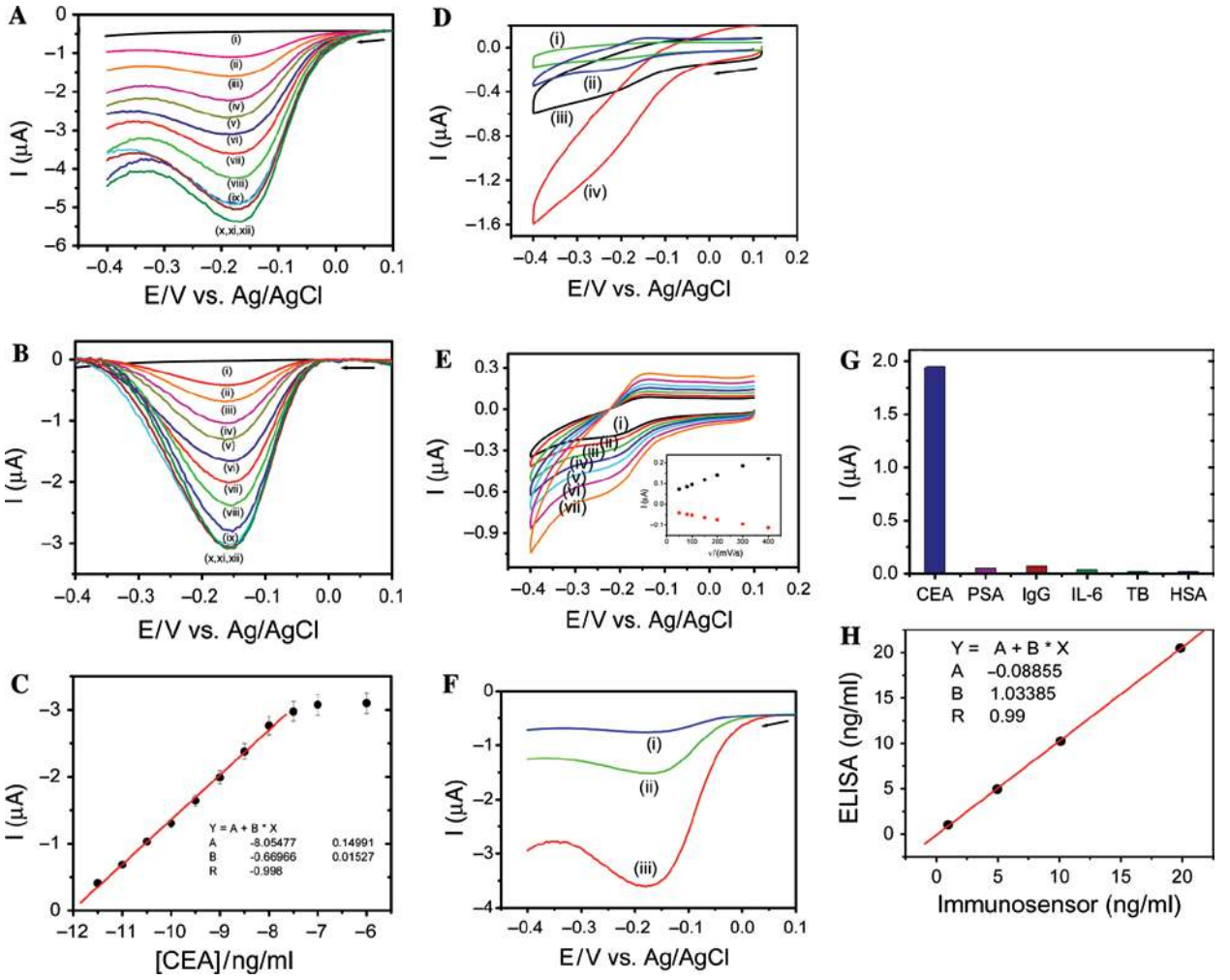

Figure 2: Electrochemical measurements of CEA immunosensor (A) recorded responses of square wave voltammetry (SWV) responses obtained for Au/Cys/Den/AuNP/Th-based CEA immunosensors at (i) blank noise and at different concentrations of CEA: (ii) 10 pg/ml to (xii) 1.0 μg/ml. (B) Responses of SWV with subtracted background and (C) the related calibration plot. (D) Recorded responses of CV obtained for Au/Cys/Den/Th-based (i, iii) as well as Au/Cys/Den/AuNPs/Th-based (ii, iv) CEA immunosensors in a PBS solution of 0.1 M in the absence (i, ii) or presence (iii, iv) of 1.0 mM glucose. (E) Recorded currents of redox peaks vs. scan rate dependence and (F) recorded responses of SWV for Au/Cys/Den/AuNPs/Th-based CEA immunosensor in a PBS solution of 0.1 M (i) and in a glucose solution of 1.0 mM in the presence of (ii) Au/Cys/Den/Th- and (iii) Au/Cys/Den/AuNP/Th-based CEA immunosensors. (G) The bar graph compares SWV responses of Au/Cys/Den/AuNP/Th-based immunosensors toward CEA and other proteins, which reveals high selectivity of the sensor, and (H) the correlation response plot between the immunosensor and ELISA methods, which proved the agreement between two approaches. Reprinted with permission from Ref. [79]; copyright 2013, American Chemical Society.

signal probe (SH-SP) was prepared as double-stranded DNA and incubated with streptavidin-coated magnetic dynabeads (STV-MB). (2) When adenosine bound to the conjugate, STV-MB/biotin-ABA/SH-SP, the RNA duplex was dehybridized, leading to the release of signal probe. This single strand was captured on thiol capture probe (CH-SP) by DNA complementary hybridization. (3) AuNPs were bound to the thiol ending of SH-SP. These particles provided a large surface area for many electroactive thionine molecules to bind. (4) DPV detection produced an amplified current related to thionine-decorated AuNP, which was proportional to the amount of the released SH-SP and to the amount of adenosine.

2.1.4 DNA-based metallic nanobiosensors

DNA biosensors incorporate a single-stranded DNA as a probe that has affinity toward a specific DNA sequence of the target DNA molecule (complementary strand), and it is often used to detect genetic disorders related to DNA mutation. Electrochemical DNA biosensors are preferred

due to their capability for miniaturization [88]. Wang et al. [89] reported a novel electrochemical DNA sensor for determination of the BCR/ABI fusion gene related to chronic myelogenous leukemia. AuNPs were attached to a modified carbon glassy electrode surface to immobilize many capture probes and amplify the signal. The electrochemical impedance spectroscopy (EIS), the cyclic voltammetry, and DPV approaches were applied to measure the samples. A low detection limit of 2.11 pm and satisfying reproducibility were achieved by the biosensor.

Another interesting recent modification for DNA biosensors was proposed by Huang et al. [63]. With a suitable process, AuNPs were attached to a tungsten sulfide-graphene (WS_2) nanocomposite-modified electrode. Then, the thiolated ssDNA probe, was immobilized on AuNPs via Au-S bond formation. The sensor was used to detect DNA related to dengue virus through a decrease in the voltammetry reduction current of a redox indicator as a consequence of the DNA hybridization event. Satisfactory electrochemical behaviors were obtained, and the complementary DNA was detected in femtomolar concentrations owing to synergistic signal amplification effect of WS_2 and AuNPs.

2.1.5 Electrochemical cytosensors

In 1990, cytosensors were invented by administration of silicon technology, and the microphysiometer biosensing system emerged [90]. The microphysiometer cytosensor device based on light addressable poteniometry was designed to study cell responses to several external stimuli such as chemicals and toxicants through the living cell energy-dependant pathways by monitoring the rate of glucose and oxygen uptake, heat production, pH, and extracellular acidification rate [91, 92].

Cytosensing systems have been extensively combined with electrochemical methods due to simple instrumentation and low time and cost requirements [93]. Biofunctionalized NPs with recognizer biomolecules, which combine the specificity of biomolecules with the signal amplifying properties of NPs, can be utilized to obtain highly sensitive electrochemical cytosensing [94]. By evolution of electrochemical cytosensors, a variety of cytosensors and biomaterial interfaces have been designed in order to immobilize cells and evaluate cell surface carbohydrates and glycoproteins, as changes in their expression may signal various diseases, especially cancer [95, 96]. Also, many investigations have been carried out to identify suitable cancer-related receptors and their specific binding recognizers. One popular example is folate receptor, since it is demonstrated that its overexpression contributes to breast cancer and liver cancer events and it can be assessed to define the stage of the disease [97]. Based on special affinity of folic acid to folate receptor, Xu et al. [98] developed a noninvasive and sensitive electrochemical cytosensor using AuNP functionalized folic acid and ferrocene as a signal indicator for detection of cancerous cells. The biofunctionalized AuNPs served as electron transfer accelerator between signal indicator and the electrode and also offered large surface area for accumulation of more ferrocenes, which in turn improved the sensitivity.

Hybrid materials with incorporation of noble MNPs have been widely investigated for cytosensing applications. One example is Au@BSA-based cytosensor; a core-shell-based 3D microsphere structure consisted of AuNP and bovine serum albumin (BSA), which was conjugated with anti-CEA antibody via glutaraldehyde, was fabricated for determination of CEA-positive tumor cells with EIS [99]. In another report, layer-by-layer assembly consisting of MWCNT, AuNPs, and polydopamine (MWCNTS@AuNPs@PDA) was constructed as immobilizing platform for Aptamer-DNA concatamer-quantum dots (QDs), as recognizing probe in electrochemical cytosensor, which exhibited high sensitivity toward cancerous cells. AuNPs were adopted to integrate the efficiency of MWCNTS due to their excellent surface reactivity, solubility, and bioactivity [31]. Cytosensor's application is mainly focused but not limited to cancer diagnosis. Some recently developed electrochemical cytosensors are listed in Table 3.

2.2 Optical biosensors

2.2.1 Plasmonic nanobiosensors

The oscillations of free electrons in the conduction band of certain metals are called plasmons, which can interact with photons of incident light to form a polaritron. Some metals, such as silver, copper, and gold, have electronic interband transitions in the visible range. The surface plasmons (SPs) interact with specific wavelengths of light in the method called SP resonance (SPR). When physiochemical changes happen in the thin surface layer of the metal such as a biorecognition event, the dielectric constant changes and leads to a change in the RI of the thin layer. This change in RI affects several spectroscopic measurements, including fluorescence, Raman scattering, and second harmonic generation. Localized SPR (LSPR) involves the more pronounced local oscillations occurring in the close vicinity (a few nm) of a MNP [110]. When the incident photon frequency is resonant with the collective

Table 3: Recently developed noble MNP-based electrochemical cytosensors.

Nanomaterial	Biorecognizer	Transduction method	Limit of Detection	Linear range	Analyte	Reference
Au@Pd core-shell NP-modified magnetic Fe_3O_4/MnO_2beads (Fe_3O_4/MnO_2/Au@Pd)	Thiolated TLS11a aptamers	Cyclic voltammetry (CV), EIS, and differential pulse voltammetry (DPV)	15 cells ml^{-1}	1×10^2–1×10^7 cells per ml	Human liver hepatocellular carcinoma cells (HepG2)	[100]
GCPE/AuNp/Cys/Glu/PAMAM/FA		CV, EIS	100 cells ml^{-1}	10^2cells per ml and 10^6 cells per ml	HeLa cells utilized as model cancer cells	[101]
The nanocomposite interface of the AuNPs/polyaniline nanofibers (AuNPs/PANI-NF)	Anti-P-glycoprotein	CV, EIS	80 cells ml^{-1}	1.6×10^2 to 1.6×10^6 cells per ml	Drug-resistant K562/ADM leukemia cells	[102]
G-quadruplex/hemin/aptamer-AuNPs-HRP	Thiolated TLS11a aptamer	DPV	30 cells ml^{-1}	1×10^2 to 1×10^7 cells ml^{-1}	Human liver hepatocellular carcinoma cells (HepG2)	[103]
Nanocomposite of PAMAM dendrimer and AuNP-decorated magnetic Fe_3O_4 beads	HRP/TRAIL	Cyclic voltammetry	~40 cells ml^{-1}	–	DR4/DR5 on the leukemia cell surfaces	[104]
Au-$RuSiO_2$ NPs	Concanavalin A (Con A)	Electrogenerated ECL	600 cells ml^{-1}	1.0×10^3 to 1.0×10^7 cells ml^{-1}	K562 cells	[105]
AUNPs-doped polyaniline nanofiber (Au/PANI-NFs) composite	Anti-CD antibody	EIS	1×10^4 cells ml^{-1}	–	T-cell	[106]
AuNPs/GO-PANI-NF	Abt1 aptamer and epidermal growth factor (EGF)-funtionalized CdS QDs (CdSQDs)-capped magnetic bead (MB)	Electrochemiluminescence	40 cells ml^{-1}	80 to 4×10^6 cells ml^{-1}	MCF-7 cell	[107]
AuNP-decorated MAPR (AuNPs/MAPR) microspheres	EGFR antibody	Square wave voltammetry	5 cells per ml	–	Lung cancer cells (A549 cells)	[108]
cDNA-AuNP nanoconjugates	Aptamer-Fe_3O_4 MNPs	Square wave anodic stripping voltammetriy (SWASV)	10 cells per ml		CCRF-CEM leukemia cells	[109]

oscillation of the free electrons in the conduction band of the MNPs, the LSPs undergo wavelength selective adsorption in the ultraviolet (UV)-Vis region [111]. Methods utilized for LSPR sensing are generally colorimetric sensing, RI sensing, and bulk RI sensing [112]. In more recent papers, RI sensing is the most common method employed.

In order to enhance LSPR and make it suitable for bioapplications, size tuning of the noble MNPs is a beneficial although limited strategy. It is desirable to select appropriate NP sizes to achieve higher detection sensitivity as a result of higher shifts in response to small RI changes due to the bio-recognition process. The plasmon shift per RI unit (RIU) change is used to describe the enhanced plasmonic sensitivity. The highest value for gold nanospheres is approximately 70 nm/RIU for a 30-nm particle size. In addition, sensitivity can be improved by increasing the particle volume to some optimum level. Since nanostructure geometries other than nanospheres offer plasmon resonance tunability, they can be used to achieve high plasmon sensitivity, which is called "shape tuning." For instance, by changing the shape from spherical to rod shaped, two resonances will be observed along short and long nanorod axis, and by increasing the length-to-width ratio, the long-axis LSPR red-shifts from the visible to the near infrared (NIR) and the oscillator strength increases. Using core-shell structures is another approach, in which the decrease in shell thickness leads to the LSPR to be red-shifted from the visible to the NIR as a result of an increase in coupling between the inner and outer shell SPs. And with a decrease in the shell thickness-to-core size, the LSPR frequency decreases semiexponentially and the plasmon sensitivity is also improved [113]. The plasmonic features of various metallic nanostructures have been studied extensively over the past decades, and unique nanomaterials with highly enhanced surface sensitivity have been engineered for biosensing applications. Various geometrical shapes of the actual NPs (stars, pyramids, triangular, prisms, etc.) have been reported for optimum LSPR. As expected, the LSPR of anisotropic NPs, such as triangular NPs, has been proven to be more sensitive to RI changes due to their sharper tips or edges, compared to spherical NPs, since they generate hotspots with higher dipolar fields on their edges [114–118].

A prism-based periodic gold nanohole array sensor was fabricated and the propagation of different possible plasmon modes was investigated in the NIR region [119]. Since SPR sensitivity is related to excitation wavelength, measurements in this area with long excitation wavelengths were more sensitive. Both sample-sensitive and non-sample-sensitive Bragg SPs were demonstrated using different dielectric media by means of SPR spectroscopy. The surface parameters, such as periodicity, nanohole diameter, and excitation wavelength, can be tailored to get the best surface sensitivity compared to a continuous gold surface. To enhance the SPR performance of these nanohole arrays, a theoretical study was conducted to simulate the effect of dielectrophoretic force by applying an AC signal between the coated glass electrode and the gold nanohole arrays. The results revealed the potential of this methodology due to better diffusion, and aggregation of analyte molecules toward the edges of each individual nanohole (Figure 3) [120]. In another recent study, gold bipyramidal NPs were used to construct an antigen detecting SPR biosensor due to its SPR signal-enhancing feature and led to remarkable RI changes and a desirable shift in wavelength. These bipyramids proved to be more efficient than Au nanorods because of their sharper tips [40]. Au nanocage (AuNC) is another interesting anisotropic form of AuNPs with a higher area of binding surface. It has demonstrated a lower limit of detection and improved sensitivity even compared to AuNPs when employed in a biotin-specific optical biosensor using a tilted fiber Bragg grating transducer. This advantage was attributed to the geometry providing flat contact surfaces in the AuNC structure [121].

The cutoff wavelength measured in the spectra was used to detect the molecular recognition event by comparing both the peak intensity and wavelength shifts. Some other practical SPR-based biosensors have been developed employing various metallic nanostructures for different applications. Examples are gold nanostars functionalized with DNA to form a biosensor capable of detecting DNA hybridization events based on SPR spectroscopy [122] and DNA biosensor capable of isothermal identification of pathogenic microorganisms [123]. Recently, several SPR-based aptamer-based sensors have been proposed based on AuNPs as signal amplifiers [124–126].

Some novel LSPR optical fiber biosensors have been reported using the LSPR properties of Au and Ag nanospheres [127], nanometal rings and nanometal gears [128], and plain AuNPs [129]. The first study detected gastric cancer biomarkers by using a dip fiber. The second study focused on simulation methods in order to design and analyze optical LSPR based on nanometal rings and gears, and the third study used a U-bend fiber sensor for detecting explosive vapors.

In addition to Ag and Au, palladium (Pd) has also been proved to be quite amenable for LSPR sensing in Au/Pd core-shell form and could even be more sensitive to RI changes compared with AuNSs and AgNSs [41].

Aluminum is another highly advantageous metal for optical biosensing in the UV range where many peptides

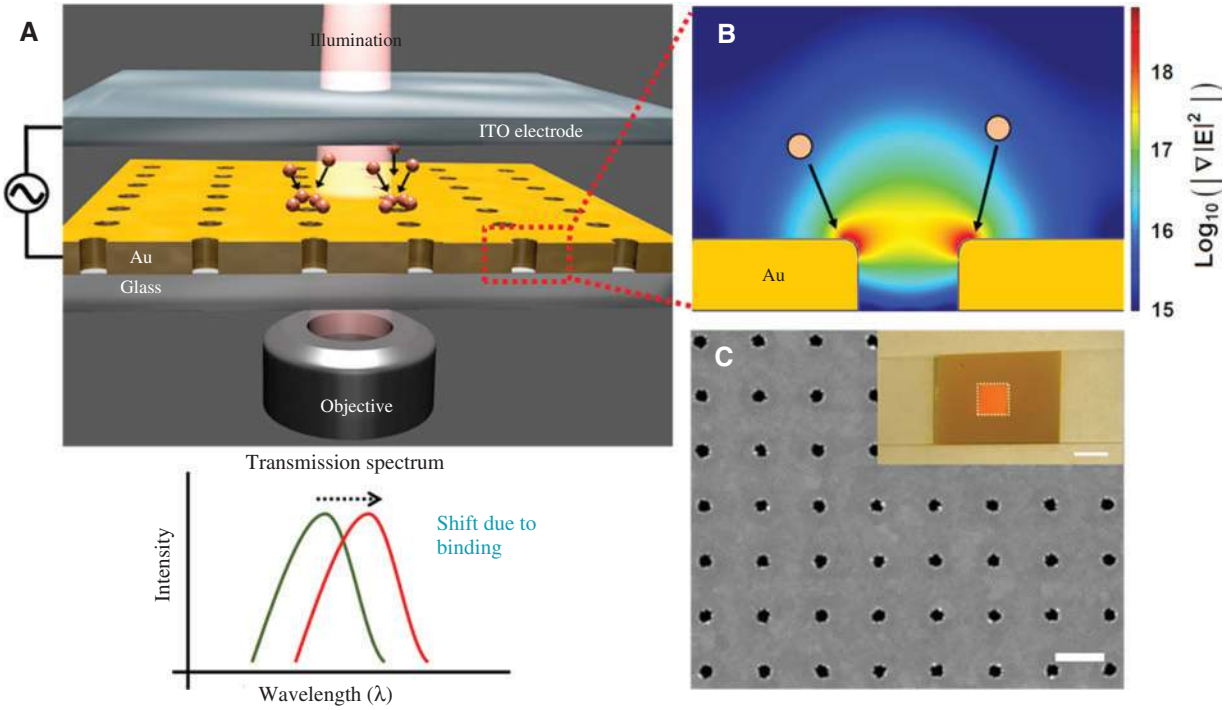

Figure 3: (A) Illustration of the setup used for the dielectrophoretic concentration of analyte molecules. Upon applying appropriate bias between the upper ITO electrode and gold nanohole array, analyte molecules got attracted toward the gold surface. In the setup, a tungsten-halogen lamp was used to illuminate the setup, and the light transmitted through the nanohole array was collected. Because of analyte binding, the transmission spectrum related to the SPs at the interface of gold-water shifted toward longer wavelengths due to changes at the interfacial RI. (B) Analyte molecules were attracted toward the hole edges, where the electric field with strongest intensity gradient existed (red color) along the rims of the holes. (C) SEM image of the nanohole array was used to measure the hole diameters: hole diameter and periodicity were 140 and 600 nm, respectively. Scale bar is 500 nm. Inset: photograph of the template-stripped gold nanohole array. Scale bar is 0.5 μM (scale bar in inset image is 1 cm). Adapted from Ref. [120]; American Chemical Society.

and proteins absorb UV light, since SPR resonance cannot be observed for noble metals like Au and Ag at wavelengths shorter than 500 nm. It has been shown that a "nanoconcave" particle shape led to an increase in RI sensitivity of the Al arrays due to an increase in the pitch [130]. Anodic porous alumina has also been investigated for its potential to be a suitable substrate for plasmonic spectroscopy, especially surface enhanced Raman spectroscopy. A recent study revealed good biocompatibility of this material for live cell optical sensing [70]. In a similar report, a biosensor based on nanoporous anodic alumina rugate filters was constructed, and its optical sensing performance toward D-glucose molecules was investigated by reflection spectroscopy. The observed shifts in characteristic peaks after filling the rugates with D-glucose was attributed to RI changes as well as changes in other parameters. Good linearity together with low detection limit of 0.01 M of D-glucose (i.e. 1.80 ppm) was achieved with the proposed structure [131].

Several LSPR biosensors have been reported in recent years with the aim to improve previous studies by modifications made on the substrate materials or increasing the diversity of the NPs [132–134].

It is indicated that MNP assemblies display distance-dependent plasmon resonances as a result of field coupling [113]. There are recent studies on developing controlled orientational NP assemblies, which exhibit interesting optical activity due to massive electron oscillations compared to individual NPs, and their applications in biosensing field are under investigation. However, the applications of orientational NP assemblies for optical sensors should be improved in terms of specificity, sensitivity, and repeatability to reach commercial applications on real samples [135].

2.2.2 Fluorescence biosensors

The fluorescence phenomenon is a successive process consisting of the absorption that occurs after incoming photon of light excites the fluorescence-responsive molecule to a higher vibrational state; the vibrational

relaxation to the lowest energy level; and the emission of a photon with longer wavelength accompanied by the molecule's return to the ground state [136]. Several parameters may be assessed as an analytical signal such as emission intensity, emission wavelength, lifetime, etc., which may result from alterations that affect the concentration of fluorescent agent or any changes that influences its emission [137].

Owing to the SPR features, which offer unique tunable absorption and scattering properties for noble MNPs, they can be employed as the alternatives for conventional fluorophore dyes for fluorescence-based biosensing and imaging purposes. For instance, it is indicated that a single 40-nm AuNP exhibits scattering with intensity equal to the intensity measured for approximately 10^4 fluorescein molecules [138]. Additionally, noble MNPs have been vastly investigated to enhance the spectral properties of fluorophores via an interaction between the excited-state fluorophore and SP electrons of noble MNPs. These interactions are summarized under the titles of metal-enhanced or surface-enhanced fluorescence and radiative decay engineering. Coupling the MNPs to the fluorescent emitters leads to fluorophore quenching in close proximity (0–5 nm), spatial changes in incident light field, and alterations in the speed of radiative decay, which is related to the life time of the fluorophore [139].

The quenching strategy has been implemented to develop numerous fluorescent-based "on-off" biosensors based on extremely high quenching efficiency (as much as 99%) of AuNPs [140]. Quenching is obtained through Forster resonance energy transfer (FRET) mechanism. When a strong quencher agent such as AuNp, which plays the role of accepter, is placed in close distance with fluorophore molecule as a donor, the excited fluorophore transfers energy to the accepter via nonradiative dipole-dipole coupling. The transfer efficiency between FRET pair depends on the orientation and distance between the FRET pair and the overlap of absorption spectra of the acceptor and the emission spectra of the donor [141]. Shamsipur et al. [142] developed fluorescence biosensor based on the quenching ability of AuNPs for determination of DNA hybridization. Upon adding the complementary target DNA to the solution containing probe DNA-functionalized AuNPs and bis(8-hydroxyquinoline-5-solphonate) cerium(III) chloride as fluorescent probe, the quenching of the fluorophore agent was observed so that the quenching intensity was proportional to the concentration of the target DNA. In a study toward environment pollutants, Huang et al. [143] developed biosensor for determination of Hg^{2+}, employing AuNP-functionalized 10-mer single-stranded DNA as a quencher and QD (Mn : CdS/ZnS) fluorophore. In the absence of Hg^{2+}, due to the hybridization of DNA strands, a plunge in fluorescence was observed, while the presence of Hg^{2+} induced conformational changes to the fluorophore-tagged DNA, resulting in release of the AuNP-functionalized DNA, which in turn restored the fluorescence. Recently, several studies have been conducted to develop fluorescence-based biosensors exploiting quenching effects of noble metal nanostructures for cancer diagnosis.

Zhu et al. [144] fabricated gold triangular nanoplates with silver coating for detection of CEA, a prominent cancer biomarker, by a fluorescence spectroscopy assay, through quenching the fluorescence emission of CEA by the proposed nanostructure. It was observed that the quenching intensity increased with the thickness of silver coating and the concentration of CEA. In another recent study, Jeong et al. [145] developed GO/AuNP nanocomposite and fluorophore-labeled aptamer for detection of CD44, a cancer biomarker, based on the fluorescence quenching ability of the nanocomposite.

Apart from the quenching effect, MNPs have been employed to enhance the fluorescence emission of the fluorophore as a base for biomolecule and chemical detection.

The nature of the induced plasmons on the metal surface and radiation factor determine whether quenching or enhancement takes place. The absorbance of the metal colloids while they are positioned in specific near distance with the fluorophore molecule is responsible for fluorescence quenching since the metal particles cannot radiate in near-field interactions, whereas the scattering of these particles due to far-field interactions of metal-fluorophore leads to the fluorescence enhancement of the fluorophore [146]. Tang et al. [147] developed a fluorescence-based glucose biosensor based on enhancement effects of AgNPs on CdSe QDs. The AgNPs-CdSe QD complex demonstrated a ninefold enhancement in fluorescence compared to CdSe alone. The results revealed 1.86 mM low detection limit and 2–52 mM linear range. Xu et al. [148] studied fluorescence enhancement of AuNCs and AuNRs for cancer imaging and sensing by conjugating these nanostructures with sulfonated aluminum phthalocyanine (AlPcS) as a fluorophore, which was used for cancer therapy. The reported enhancing factors for AlPcS-AuNRs and AlPcS-AuNCs were 6 and 150, respectively. Several recent studies have addressed metal-enhancement fluorescence technique for sensitive sensing of various analytes by tuning the size and shape of noble MNPs and evaluating different classes of fluorophores, such as organic dyes and QDs.

2.2.3 Chemiluminescence and electrogenerated chemiluminescence biosensors

Chemiluminescence (CL) is light accompanied by chemical reaction in which the electrochemically excited product is formed, and this product emits light upon returning to the ground state. This phenomenon has been applied for detection purposes when one of the reactants can be linked to the analyte, and the magnitude of light output is proportional to the concentration of species to be determined [149]. Zhang et al. [150] reported the direct usage of colloidal AuNPs on the CL for the first time. They found that AuNPs with a size regime from 6 to 99 nm could enhance the CL from the luminol-H_2O_2 system. Some noble MNPs, especially colloidal AuNPs, have been served as the carrier of biological recognizing agent and signal amplifying label in many CL-based determinations. Since colloidal AuNPs can (1) be easily prepared in a wide range of size, (2) retain the biochemical activity of the labeled biomolecules due to their biocompatiblity, and (3) be easily visualized by transmission electron microscopy, they have been frequently utilized as labels in biotechnological systems [151].

The high detectability of the luminescence analytical signal makes it suitable for developing miniaturized bioanalytical devices for many biotechnological applications, especially to perform the high-throughput screening of genes and proteins in small sample volumes [152]. Another luminescent-based technique, electrogenerated CL (ECL), has demonstrated promising advantages such as simplicity, high sensitivity, rapidity, and easy controllability [153]. ECL is the process in which the species generated at electrodes undergo high-energy-electron transfer because of electrochemically initiated reaction, and these excited species emit light after relaxation. The luminescence in ECL can be controlled by altering the applied potential and the time, to delay the emission until biorecognition takes place [154, 155].

2.2.3.1 Immunosensors

Several CL immunoassays have been designed by incorporating AuNP labels. Bi et al. [156] proposed CL sandwich-type immunoassay for determination of AFP tumor marker by employing anti-AFP immobilized magnetic beads (MBs) and HRP-labeled anti-AFP antibody conjugated with AuNP. As expected, luminol-H_2O_2-HRP-bromophenol blue (enhancer) reaction generated highly enhanced CL signals. The comparative results revealed that detection limit was one order of magnitude lower than the same assay without using AuNP label. A recent CL immunosensor is proposed by Sabouri et al. [29], to detect the hepatitis B surface antigen. The CL label was prepared by covalent immobilizing anti-HBSAg as the second antibody and luminol on AuNP surface. The antigen was detected through sandwich immunoassay between the first antibody in the presence of H_2O_2 and Au^{3+} as catalyst and the antigen and second labeled antibody. A growth in CL signal by an increase in analyte concentration and secondary antibody was observed.

Due to disadvantages of labeling procedure, such as being complex, costly, and time-consuming and also yielding narrow linear range and unsatisfying detection limits, efforts have been put into designing label-free CL immunosensors. Yang et al. [157] have fabricated label-free CL immunoassay for detection of human immunoglobin G (HIgG) based on a decrease in CL signal due to immunocomplex formation that prevented luminol-H_2O_2-PIP to reach HRP sites on HRP-AUNP-chitosan combination (Figure 4).

Besides the popular application of AuNPs as antibody immobilizer, it has been proved that AuNPs could catalyze the ECL activity of ECL labels such as *N*-(aminobutyl)-*N*-ehylisoluminol (ABEI) [34]. Here, AuNP was applied to trap and store electrons from the conductive band of graphite-like carbon nitride nanosheets g-C_3N_4NSs ECL active substrate and to catalyze persulfate (coreactant) reduction in a label-free CEA immunoassay. It was

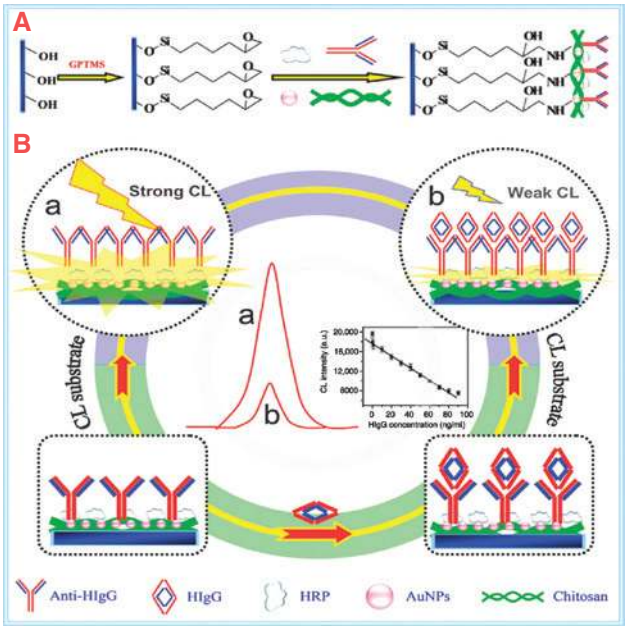

Figure 4: Schematic of the preparation method of the immunosensor and label-free chemiluminescent immunoassay of HIgG. Reprinted with permission from Ref. [157]; copyright 2015, Royal Society of Chemistry.

indicated that the combination of AuNPs with g-C_3N_4 resolved the passivation issue in the ECL of g-C_3N_4 and the overinjection of highly energetic electrons by an increase in potential beyond −0.9 V, which prevents the ECL emission [158]. Wang et al. [159] have developed immunosensor for carbohydrate antigen (CA 15-3) by utilizing a combination of Ru(ll) luminophore and poly(ethylenimine) (PEI) as a coreactant in the same molecular structure, grafted on palladium nanocages (PdNCs). PdNCs, owing to its good electrocatalytic activity and high specific surface area and special structure with porous walls and hollow interior, were used to load abundant PEI, and the generated hybrid was used to decorate with $Ru(bpy)_2(5\text{-}NH_2\text{-}1,10Phen)\ Cl_2$. On the other hand, AuNP functionalized graphene implemented as substrate to immobilize the first antibody. The fabricated biosensor exhibited a linear range of 0.01–120 Uml^{-1} and low detection limit of 0.003 Uml^{-1}.

In a recent study, a solid state $Ru(bpy)_3^{2+}$ ECL sandwiched biosensor was developed for fetoprotein (AFP) detection based on the PEI functionalized RGO (PEI-rGO), which immobilized poly(amidoamine) (PAMAM) decorated AuNPs as second antibody carrier and Nafion-Ru-PtNP as platform for first antibody and the ECL substrate. AuNPs were used to improve the weak conductivity of PAMAM [160]. In another recent report, a competitive ECL immunoassay for clenbuterol (CLB) was proposed based on CdSe QDs as ECL probes and AuNP as platform, with a detection limit as low as 0.0084 ng/ml. The AuNPs were used to facilitate electron transfer, to improve the electrochemical reaction efficiency of QDs and $K_2S_2O_8$ (coreactant) by increasing the conductive surface area and to stabilize the ovalbumin-clenbuterol (OVA-CLB) antigen and OVA-CLB/BSA on the electrode surface [161].

2.2.3.2 Enzymatic sensors

The interactions of AuNPs and enzyme because of having similar dimensions, easy absorption of enzymes on AuNPs, the catalytic effect of AuNPs on the CL reaction of luminol in the presence of some oxidants, and the possibility of tailoring the size to achieve enhanced CL make AuNPs a favorable unit for most enzymatic CL biosensors [162]. Lin et al. [30] have developed bienzymatic glucose biosensor based on flow injection CL. AuNPs were doped into chitosan membrane to provide biocompatible enzyme immobilizing platform and to enhance luminol CL reaction. The glucose molecules were oxidized via GOD, producing H_2O_2 and gluconolacton, and subsequently, HRP catalyzed the oxidation reaction of luminol by H_2O_2, leading to enhanced CL signal. The enhanced mechanism indicated that AuNP acted as the electron transfer mediator and assisted the HRP enzyme to return to its reduced form. Zargoosh et al. [163] have developed enzymatic glucose biosensor by integrating the sensitivity of peroxyoxalate CL system and selectivity of enzymatic reaction. The H_2O_2 generated from the enzymatic oxidation of glucose reacted with peroxyoxalate and a fluorophore, and the emitted light was proportional to peroxide concentration. The carbon nanotubes (CNTs)/AuNPs in nafion film on graphite support were used to immobilize the GOD. The CNTs/AuNPs were proved to enhance the signal-to-noise ratio and improve the nafion film response. In another recent report of glucose biosensor, Chaichi et al. [35] implemented magnetic Fe_3O_4-chitosan as platform for immobilizing GOD enzyme using glutheraldehyde as cross-linking agent. It was demonstrated that AuNPs catalyzed the luminol CL reaction and offered catalytic activity toward generation of H_2O_2 as result of GOD-glucose reaction. They suggested that the enzymatic role of AuNP in the luminol-H_2O_2-AuNP system and the formation of superoxide radical, which reacted with luminol anion through electron-transfer processes on the surface of AuNP, led to the production of light emitting key intermediate (the excited state 3-aminophthalate anion); hence, the increased CL intensity was obtained. For sensitive determination of ethanol, $Ru(bpy)_3^{2+}$-based ECL was developed. Alcohol dehydrogenase enzyme (ADH) was immobilized on $Ru(bpy)_3^{2+}$-AuNP aggregates on indium tin oxide (ITO) electrode. The ennzymatic reaction of ethanol with NAD^+ via ADH yielded NADH, which reacted with $Ru(bpy)_3^{3+}$ to liberate ECL light. AuNPs served as both enzyme immobilizer through interaction between amine groups and cystein residues of enzyme and colloidal golds and the electron transfer facilitator [164]. Having such important characteristics and their dominant role in CL and ECL biosensors, several interesting studies have been carried out on enzymatic biosensors for the determination of important biomolecules by trying different shapes of AuNPs and/or support materials to achieve better efficacy. Some examples are AuNP catalyzed luminol-based cholesterol sensing ECL biosensor [36], the lactate sensing luminol and hollow AuNP-based ECL biosensor [165], and the hollow gold nanosphere catalyzed luminol-based ECL glucose biosensor [37].

2.2.3.3 Nucleic-acid-based biosensors

The CL technique has been used for sensitive detection of DNA via DNA hybridization process using NP labels. Sensitive and rapid detection of DNA with ultra-low concentration is highly essential for the detection of infectious diseases, genetic therapy, and early screening of diseases [166]. AuNPs were utilized as signal amplifying labels to immobilize several CuS NPs as the second

label. It has been demonstrated that highly stable Cu^{2+} ions, after being released in solution, take part in luminol-H_2O_2-Cu^{2+} system and offer ultrasensitive CL detection for DNA [167]. In order to improve sensitivity and specificity, hybridization chain-reaction-based amplifying strategy has been administrated, which is a chain reaction of recognition and hybridization steps between a pair of complementary, kinetically trapped hairpins, which significantly amplify short sequences of oligonucleotides. Human immunodeficiency virus type 1 was detected by applying a similar strategy using ECL with a low detection limit of 5.0 fM. After hybridization of target DNA with capture probe, and adding DNA probes (auxilary 1 and auxilary 2), the streptavidin-coated AuNPs were introduced to biotinylated DNA probes to bind through biotin-SA interactions to produce a highly amplified ECL signal through catalyzing luminol [168].

In some CL- or ECL-based biosensors, NPs are implemented not as a catalyst but as chemicals that dissolve to generate CL signal [169]. In one recent example for determination of platelet derived growth factor-BB (PDGF-BB) growth factor protein, biotinylated aptamer, the capture antibody, and the target protein formed a ternary complex, which then reacted with streptavidin-AuNPs. Subsequently, AuNPs reacted with $HAuCl_4$ and NH_2OH, which led to the catalytic deposition of gold metal onto AuNP surface, leading to its enlargement. Then, after adding HCl-Br_2 oxidative solution, AuNPs were oxidized and a large number of Au^{3+} were released to the solution, which catalyzed the luminol CL reaction. The yielded CL signal was proportional to the target concentration. A concentration as low as 60 pM could be quantified by the proposed biosensor [170].

Since the overexpression of PDGF-BB protein has been indicated in some cancer types, sensitive determination of it plays a significant role in early cancer therapy. Regarding this issue, recently, attempts have been made to develop more sensitive methods, such as a combination of rolling circle amplification strategy with the aforementioned hydroxylamine-enlarged AuNP approach, which yielded a much lower detection limit, i.e. 0.06 pM [171].

Previously, we discussed the application of MNPs in enzyme- and immunoassay-based biosensors as signal amplifiers and ECL or CL reaction catalysts. Gill et al. [172] developed CL thrombin-sensing aptasensor by using PtNPs as label. After the surface functioned thrombin aptamer captured thrombin, the PtNP-capped second aptamer bound to the target, and PtNPs catalyzed the CL generation in the presence of luminol/H_2O_2. The same group also evaluated PtNP role as a CL catalyzing label through hybridization of target DNA with its analyzing probe. In another recent study for determination of thrombin, a novel signal-off aptasensor was constructed. The AuNPs were employed as the first and second aptamer immobilizer and enhanced quenching performance by carrying several hemin molecules. The Au@CeO_2NP assembly was used to immobilize the thrombin detecting aptamer (TBA2), and hemin molecule was added to TBA2/Au@CeO_2 NP to uphold quenching effect of CeO_2NPs on $Ru(bpy)_3^{2+}$ ECL signal. While the enhanced ECL achieved as a result of thrombin capture by TBA1 aptamer anchored on nano-Au/Ru-PEI-PAA, the ECL signal was quenched after adding hemin/TBA2/Au@CeO_2NPs. The quantification of thrombin was attained by measuring the difference between two ECL intensities for different concentrations of thrombin [173].

Ding et al. [174] developed a highly sensitive ECL cytosensor based on a combination of aptamer and the developed ECL probe for detection of Ramos cells. The AuNPs tagged with linker DNA and tris (2,2′-bipyridyl)-ruthenium were used as ECL probe. Two modifications were applied on MBs. First, it was modified with aptamer to bind the ECL probe and recognize the target cell. Then, it was modified with capture DNA to be hybridized with the ECL probe, which had been released after cell recognition event. The highly amplified signal was achieved owing to the potential of AuNP to carry numerous ECL tags. The low detection limit for the cytosensor was as low as 5 cells/ml. In another interesting report of aptamer-based ECL cytosensor, AuNCs were loaded with $Ru(bpy)_3^{2+}$, and Con A as specific recognizer was attached to the assembly to obtain a unique nanoprobe. On the other hand, PtNP-dotted CNTs were implemented on the electrode to immobilize the aptamer, improve the electronic transmission, and provide a large surface area. The K562 cancer cells were detected through the sandwich-type assay with a sensitivity of 500 cells/ml [175]. Several recent studies have been conducted on ECL cytosensors by taking advantage of AuNPs to carry cell recognizer or cell-specific receptors with high electron transfer capability [176, 177].

2.2.4 Photoelectrochemical biosensing

Photoelectrochemistry is a newly emerged and highly promising analytical tool that possesses characteristics of both optical and electrochemical methods [178]. The photoelectrochemical reaction involves irradiation of light from an external source, excitation of electron from valence band of photoactive material on electrode surface to the conductive band generating electron-hole pair, followed by transference of the excited state electron to the electrode

(or vice versa), and replacement of the excited state electron in conductive band by electron from external redox pair, which yields anodic or cathodic photocurrent [179]. Since charge separation and charge transfer are engaged in photocurrent production, besides light-absorbing photoelectrochemically active species, semiconductor interfaces, such as TiO_2 and SnO_2 NPs, have been applied to the electrode surface [180]. It has been reported that MNPs promote the separation of photoelectron-hole pairs and prevent their recombination. Also, these NPs improve the conductivity of the electrode [181]. Plasmonic NPs, such as AuNPs and AgNPs, based on their LSPR corresponding to collective oscillations of their surface electrons after excitation by external light, undergo charge separation and could simultaneously lend electrons to the adjacent semiconductors in the presence of proper electron donor. This mechanism has been widely used in the development of photovoltaic cells as well as biosensors [182]. It has been observed that plasmonic noble MNPs enhance the photoconversion efficiency of TiO_2 and other wide band gap semicondutors, and direct attachment of AuNPs to TiO_2 nanowires with SPR features could offer 100% increase of photocurrent density in comparison with the conventional photoelectrochemical (PEC) sensing without SPR features (Figure 5) [183].

One recent strategy for photoelectrochemical biosensing is the use of exciton-plasmon interactions (EPI) between QDs and noble MNPs [184]. A novel signal-off cytosensor was developed based on plasmon-induced resonance energy transfer between AuNP capped cysteamin and carbon dots. The affinity between folic acid and folic acid receptor in the process of Hela cell (tumor cell) capture hampered the electron transfer from ascorbic acid donor to the electrode and led to a decrease in PEC signal [185] (Figure 6A). Zhao et al. [186] proposed AgNPs and CdS QDs as EPI pair with DNA as a spacer in a photoelectrochemical system. It was indicated that AgNPs own stronger plasmon resonance (compared to AuNPs) and it fully overlaps with the adsorption band of CdS QDs (Figure 6B).

Several photoactive nanocomposites have been developed for PEC biosensing applications. The porphyrin decorated AuNP/graphene nanocomposite demonstrated good photoelectrochemical responses for oxidation of HQ, owing to the excellent electrical conductivity of graphene and the ability of AuNPs in capturing and transporting the photo excited electrons. A detection limit as low as 4.6 nM was achieved by this approach toward HQ detection [187]. In another recent report, enzymatic PEC biosensor was developed toward H_2O_2 detection. AuNP-PTA-TiO_2 nanotube scaffold was proposed as a photoactive platform to immobilize the thiolated HRP redox enzyme. The whole assembly was attached to the electrode surface by nafion and the hydrophobic ionic liquid ([Demim] Br). TiO_2 nanotubes exhibited improved performance, having a higher surface area compared to TiO_2 NPs. Also, PTA; $PW_{12}O^{3-}_{40}$, which linked AuNPs to TiO2 nanotubes, accelerated the electron transfer between the enzyme and electrode [188].

In a different strategy, AuNPs were implemented as aptamer carrier PEC nanoprobe in a signal-on thrombin sensing biosensor instead of being attached to a semiconductor. After the recognition event, PEC nanoprobe was removed and the PEC signal was restored in graphene-QD CdS nanocomposite. AuNP served as an aptamer recognizer, a viologen quencher carrier, and an energy transferring agent in the dual-quenched strategy. Also, a reverse relationship was observed for AuNP size and PEC quenching effect [189]. In another signal-on approach, Zhao et al. [190] utilized DNA hybridization and then conformational change of double-stranded DNA for PEC detection of Hg^{2+}. The rhodamine-capped probe DNA immobilized on TiO_2/CdS structure and the AuNP immobilized target DNA were employed for this approach. The disruption in exciton energy transfer between AuNP and CdS as a result of Hg^{2+} binding led to an increase in photocurrent.

According to the rapid progress in the PEC field, it is expected to extend the applications of this tool in construction of future biosensors.

2.2.5 Colorimetric biosensors

The colorimetric assay is based on visual sensing of optical changes caused by the aggregation of the functionalized MNPs in the presence of specific analyte and has a wide range of applications ranging from environmental detection of toxic metals [17], to clinical diagnosis of analytes, such as glucose [191, 192], cancer biomarkers [193], and even viruses [194]. Figure 7 illustrates preparation of the GQDS/AgNP hybrid and colorimetric glucose detection process based on the color change of the hybrid. The biosensor can be utilized for ultrasensitive detection of H_2O_2 with detection limit as low as 33 nM. The color change occurs when MNPs experience interparticle plasmon coupling as a result of aggregation or dispersion of these NPs in solution or suspension [191]. For instance, in the colorimetric detection of mercury (Hg^{2+}), 4-mercaptophenylboronic acid (MPBA) was used as an aggregation agent that can bind to AuNPs by forming Au-S bonds and cause a blue color change. AuNPs are ruby red in color, when dispersed in solution. Upon adding Hg^{2+} and MPBA, the Hg^{2+} ions compete with AuNPs, and the thiolate groups of MPBA bind to Hg^{2+}, and the solution color remains red indicating the dispersion of AuNPs. The measured absorption ratio

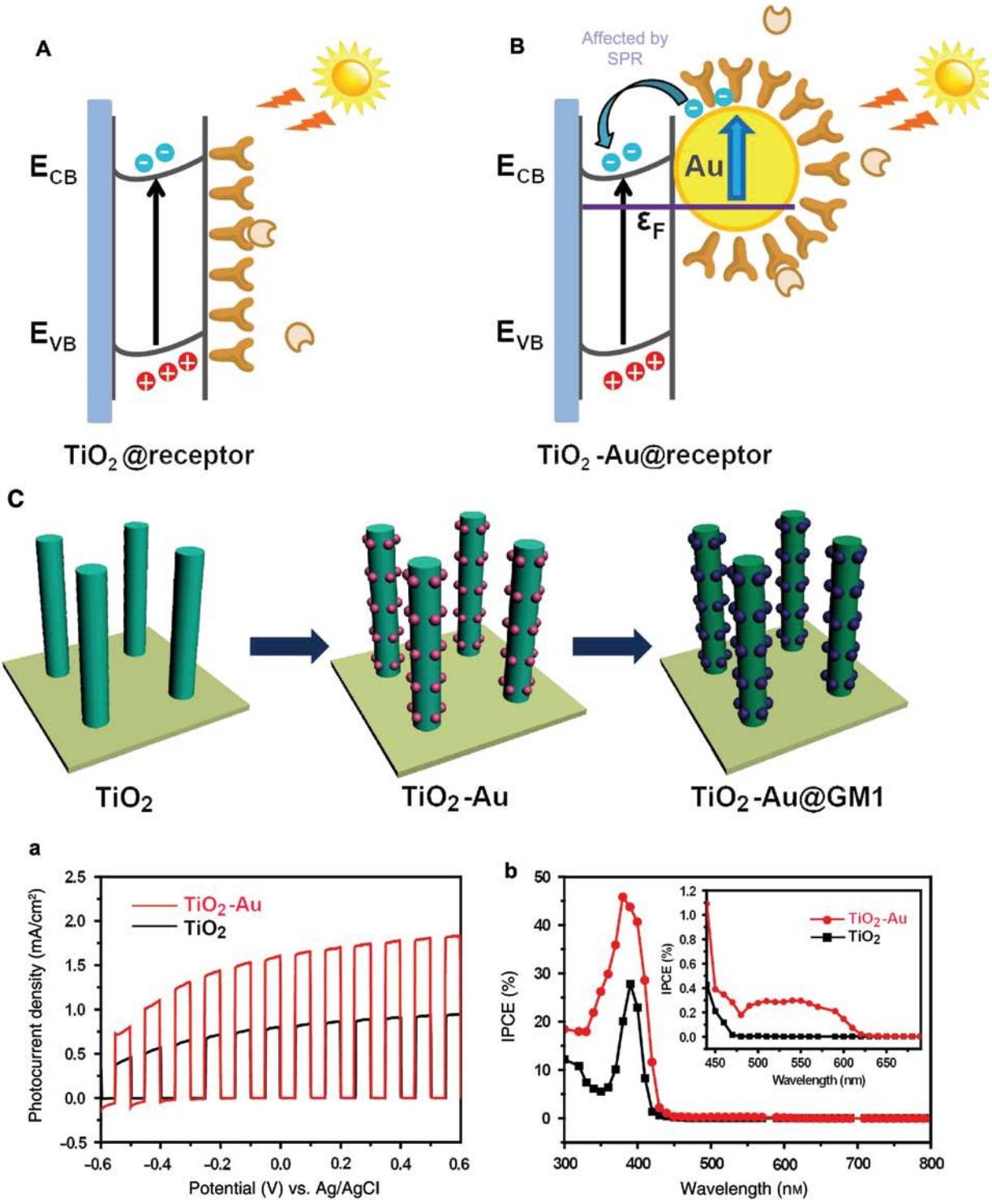

Figure 5: Schematic illustrating a comparison between PEC sensing in conventional and Au NP SPR-enhanced procedures: (A) surface receptor functionalization (GM1) as well as molecular target binding on TiO_2 sensor surfaces. (B) Au NP decoration of a TiO_2 PEC sensor, in which the surface receptor functionalization (GM1) is applied on the surface of Au NP. The molecular target binding to the receptor leads to efficacious tuning of the energy coupling and charge transfer across the Au and TiO_2 interface. (C) Preparation of TiO_2 NW-decorated Au NPs and subsequent surface modification of Au surface with ganglioside GM1. Plots: (a) Comparison of photocurrent densities of Au NP-decorated TiO_2 NWs (red curve) and pristine TiO_2 NWs (black curve) and TiO_2 NWs decorated with Au NP (red curve), related to on/off cycles of simulated sunlight illumination, which reveals higher photoactivity of TiO_2-Au NW. (b) The incident photon to converted electron (IPCE) spectrum obtained for pristine TiO_2 NWs and TiO_2 NWs decorated with Au in wavelength range tuned between 300 and 800 nm at 0.23 V against Ag/AgCl. As can be seen, there was a lower maximum value of ~28% at 390 for pristine in comparison with TiO_2 NWs decorated with Au. Reprinted with permission from Ref. [183]; copyright 2014, American Chemical Society.

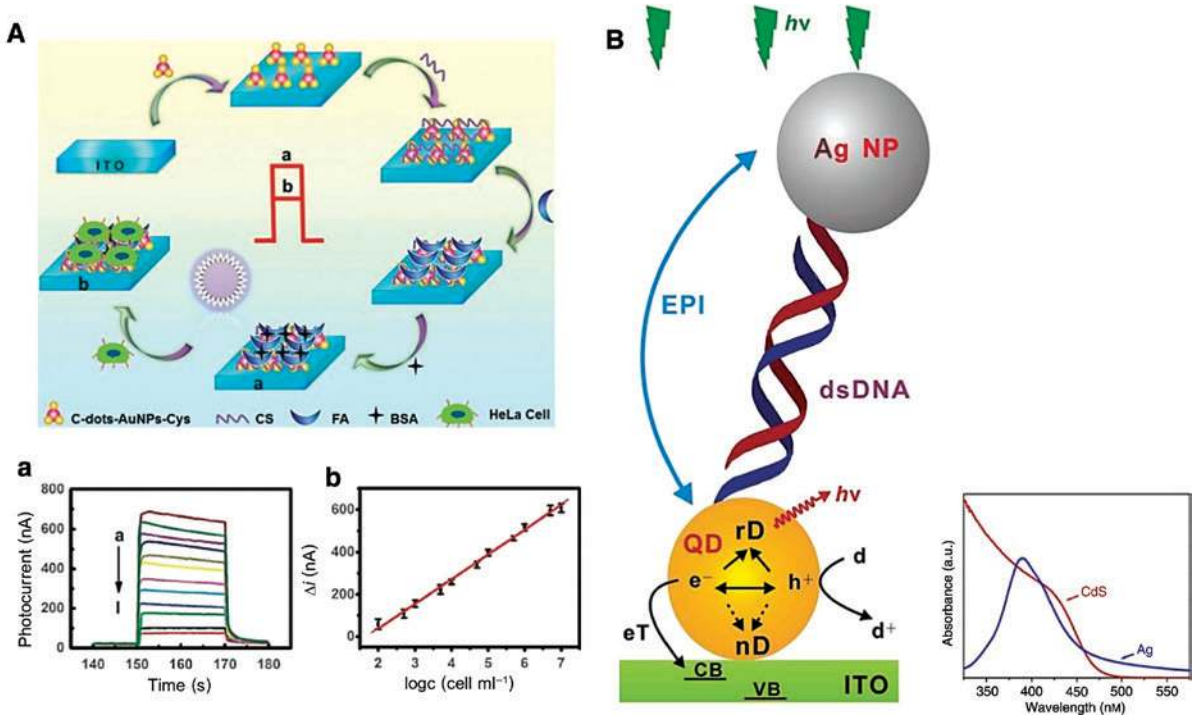

Figure 6: (A) Schematic representing the label-free ultrasensitive PEC cytosensors based on C-dots-AuNPs-Cys before (a) and after (b) capturing HeLa cells. Plots: PEC responses obtained from the cytosensor for various concentrations of HeLa cells from 0.1×10^2 to 1×10^7 (a–i) cell ml^{-1} and the corresponding calibration curve. Reprinted with permission from Ref. [185]. Copyright 2012; American Chemical Society. (B) Illustration of PEC between QDs and AgNPs bridged with dsDNA. The PEC involved several steps of light irradiation: photon absorption, which led to electron excitation of QDs, thus generation of electron-hole pair; hole scavenging by means of electron donor (d); electron transfer (eT), which could be collected by the electrode for electronic readout; recombination of electron-hole pair comprised of nonradiative decay (nD) and radiative decay (rD), followed by spontaneous emission and, lastly, EPI between Ag NP and CdS QD. The produced photocurrent signal was used for analysis. Plot: The UV-Vis absorption spectrum of the Ag NPs synthesized in aqueous solution (blue) and the fabricated CdS QDs (red). Reprinted with permission from Ref. [186]; copyright 2012, American Chemical Society.

was proportional to Hg^{2+} concentration in the range 0.01–5 μM [195]. There are some recently developed MNP-based colorimetric biosensors along with the mechanism of colorimetric assay for some environmentally toxic inorganic elements and biological analytes in Table 4.

2.3 Piezoelectric nanobiosensors

A piezoelectric sensor consists of a piezoelectric material (usually a crystal), which undergoes mechanical deformation and displacement of electrical charge when pressure is applied to its surface, or vice versa when pressure is reduced [208]. The quartz crystal microbalance (QCM) is the most popular piezoelectric detector and works based on sending an electrical signal through a gold-plated quartz crystal with a biorecognition element on its surface. When binding occurs, the mass change produces vibrations in the crystal, and the frequency of oscillation in the crystal changes [209]. MNPs have been studied for their ability to amplify signals and enhance sensitivity in several types of piezoelectric biosensors.

The potential of QCM-based immunosensors has been studied for various environmental and healthcare applications, such as monitoring foodborne pathogens and toxins. A novel QCM-based immunosensor with noble MNP enhancement was investigated for monitoring *Escherichia coli* O157 : H7 in food samples by employing antibody-NP conjugates as the detection complex. Conjugating antibodies with AuNPs as signal amplifier and employing brain heart infusion broth as growth medium to enrich the bacteria significantly improved the sensitivity of the sensor, and a detection limit of 0–10 log CFU/ml was obtained [210].

The QCM system also can be applied in label-free biomarker detection. Recently, a biosensor was developed aiming at the determination of a marker of lymphoblastic leukemia (the antigen CD10) in which glutathione-capped AuNPs were attached to the second antibody and increased the mass on the crystal surface [38]. Modified

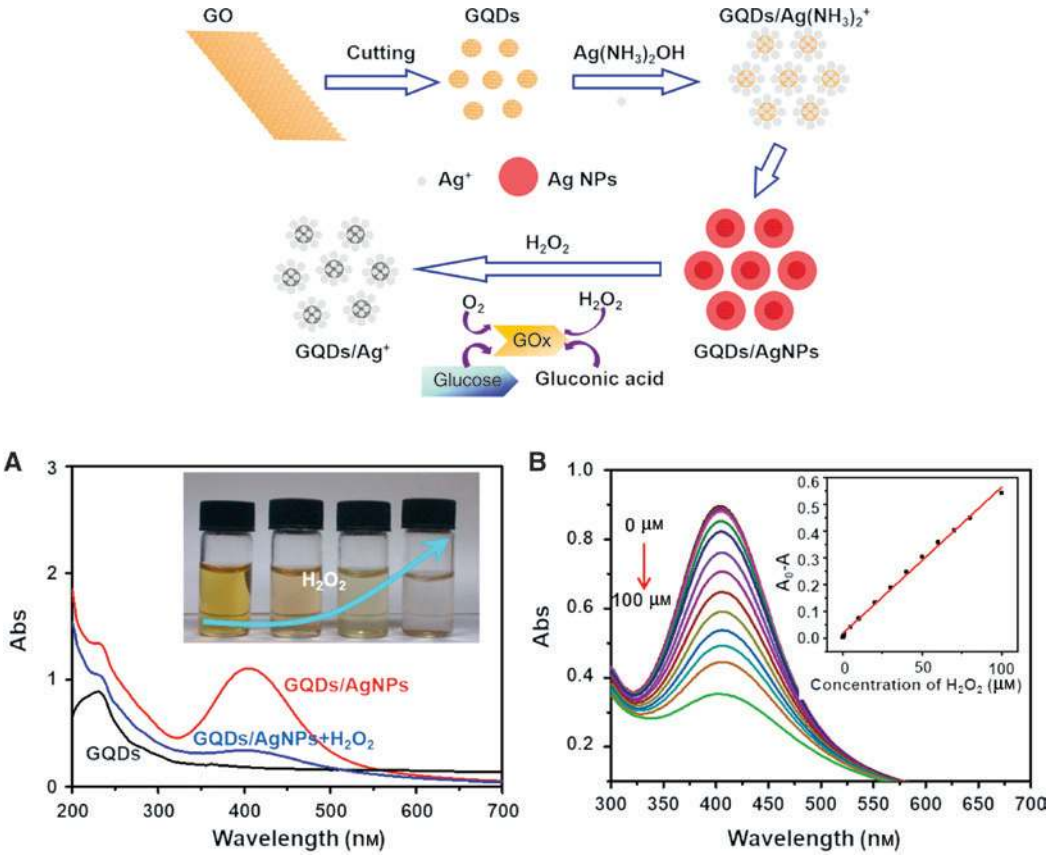

Figure 7: Schematic representing stepwise fabrication of GQDs/AgNPs hybrid and detection of the H_2O_2 and glucose based on color fading of the hybrid. Plots: (A) UV-Vis absorption spectra for 0.02 mg ml^{-1} GQDs, 0.02 mg ml^{-1} GQDs/AgNPs hybrid, and 0.02 mg ml^{-1} GQDs/AgNPs + 100 μM H_2O_2 system (the inset indicates the GQDs/AgNPs hybrid in different H_2O_2 concentrations). (B) UV-Vis absorption spectra of GQDs/AgNPs hybrid by exposing with 0–100 μM H_2O_2 (the inset shows a decrease of absorbance in different concentrations of H_2O_2). Reprinted with permission from Ref. [191]; copyright 2014, American Chemical Society.

AuNPs were also used in an aptamer-based sensor to label leukemia cells. After capturing the cells on the QCM, the AuNP catalyzed Ag deposition, which led to a decrease in resonant frequency [39]. While the strategy in most piezoelectric sensors is converting an increase in mass to a signal, in the reverse strategy, the mass lost due to dissolution of AuNPs in QCM-based biosensors was utilized for Pb^{2+} detection. The Pb^{2+} ion, along with $Na_2S_2O_3$ and 2-mercaptoethanol, was employed to accelerate the leaching of Au from the electrode surface. The decrease in mass on the QCM surface was inversely related to frequency. The frequency shift in the presence and absence of Pb^{2+} was recorded and used to measure its concentration [211].

A QCM-based label-free immunosensor was fabricated for detecting lymphoblastic leukemia antigen (CD10). AuNPs acted as a mass enhancer and antibody carrier in this sandwich-type immunosensor, leading to sensitive and rapid detection. In the first stage, CD10 molecules were captured by the first antibody (Ab1) immobilized on the gold-coated crystal surface, and the frequency was recorded after being stabilized. Then, the second antibody (Ab2), which was attached to AuNPs (Ab2/AuNPs), bound to CD10 in a sandwich assay and the frequency was recorded for the stage. The frequency change was correlated to the amount of captured CD10 with Ab1 on the QCM transducer [38].

3 Conclusions and future directions

This review has mainly focused on recently developed biosensors based on noble MNPs. Only brief explanations of the mechanisms of different biomolecular recognition processes and the theory and practice of the process of signal read-outs have been provided. It is important to understand the impressive impact that engineered MNPs have made in biomedical and diagnostic applications. These applications aim to improve the sensing and detection of several important biomolecules in the biomedical

Table 4: Recently reported colorimetric nanometal based biosensors.

Material	Colorimetric mechanism	Analyte	Low detection limit	Reference
Biofunctionalized AgNPs	Different solutions of biofunctionalized AgNPs interact with these cations	Hg^{2+}, Cd^{2+} and Pb^{2+}	–	[196]
Calix[4]arene functionalized AuNPs	Aggregation of the NPs in presence of Co(II)	Co^{2+}	10^{-9} M	[197]
Fluorosurfactant-capped AgNPs	Cysteine-induced aggregation of the nonionic fluoro-surfactant capped AgNP via non-crosslinking mechanism	Cysteine	0.05 μM	[126]
AuNPs	Aggregation of AuNPs induced by melamine	Melamine	0.02 mg/l	[18]
Citrate-capped AuNPs	Anti-aggregation of citrate-capped AuNPs	Thiocyanate	1 μM	[198]
Paper-based platform with AuNPs and ssDNA sequences	Aggregation of AuNPs	Hg^{2+}	50 nM	[199]
Poly (γ-glutamic acid) functionalized AuNPs (PGA-AuNPs)	Metal-induced aggregation	Hg^{2+}	1.9 nM	[200]
AgNPs	Hg^{2+} inhibited the 6-thioguanine-induced aggregation of AgNPs	Hg^{2+}	4 nM	[201]
Calix[4]pyrrole octa-hydrazide protected AuNPs	Aggregation of CPOH-AuNPs induced by the cross-linked complexation between CPOH-AuNPs and Co(II)	Co(II)	1 nM	[202]
Au-Ag core-shell plasmonic NPs	Ag_2S formation induced color change of the single PNPs	Sulfide	50 nM	[203]
Aptamer with AuNPs	AuNP catalyzed reductive bleaching reactions of colored substrates	Thrombin	With 4-nitrophenol 91 pM and methylene blue 10 pM	[204]
Oligonucleotide and AuNPs	DNA inhibited probe 1-induced Au NP aggregation	Alkaline phosphatase and DNA	200 pM DNA	[128]
VP and ILP metal interacting ligands functionalized AgNPs	Metal ion induced aggregation of silver complexes	Cd^{2+}, Hg^{2+} and Pb^{2+}	–	[205]
Pyridine-functionalized AuNPs	Interparticle cross-linking and aggregation of modified AuNP	Cu^{2+} and Ag^{+}	–	[206]
Copper-gold alloy NPs in electrospun nylon	Aggregation of the NPs induced by ascorbic acid in the pH range of 2–7	Ascorbic acid	1.76×10^{-2} mg l^{-1}	[207]

and healthcare-related fields, especially glucose and various antigens and biomarkers. Initially, we classified elecrochemical biosensors into amperometric and voltammetric techniques as the two dominant, widely investigated mechanisms, then we categorized them according to the biological receptors employed. MNPs have a unique combination of biocompatibility, large surface area, and good conductivity and have therefore been utilized either for providing and improving the immobilizing platforms, accelerating charge transfer between the redox-enzyme and electrode, or for signal amplification purpose as labels in enzymatic sensors, immunosensors, and nucleic-acid-based biosensors. MNPs can play a role as a "mass enhancer" or carrier of biorecognition systems in piezoelectric biosensors as well. There is an application of MNPs in cytosensors ranging from immobilizing cells to constructing nanoprobes by incorporating target-specific receptors and other cell recognizers into the surface of NPs. CL and ECL biosensors in which MNPs function as labels to catalyze the reaction of luminol or other active species are a growing subgroup. The capability of AuNPs to be directly involved as catalyst not merely as labels based on oxidation and dissolution in an aqueous solution is another interesting features of these NPs.

Optical techniques such as SPR and colorimetry techniques can be greatly enhanced by the exceptional inherent optical properties of MNPs. In this regard, recent studies have focused on LSPR characteristics of various anisotropic shapes of NPs, related comparative studies, and have recently developed label-free biosensors utilizing LSPR features. The recently developed novel photoelectrochemical highly efficient biosensors exploit the plasmonic features of MNPs, such as the unique plasmon absorbance features, intensive localized electric field in the vicinity, and visible light-induced charge separation occurring at the surface, alongside their high electronic conductivity.

Future challenges in MNP-based biosensors generally include expansion of the range of different biomolecules, which can be sensed or detected by enhancing the sensitivity and providing more rapid and versatile detection methods. However, the most demanding aspect of the progress in this field is to provide more opportunities for translational application of these nanobiosensors from the laboratory to actual clinical application using real samples from real patients.

We expect to see the evolution of faster and cheaper miniaturized plasmonics-based sensor architectures, due to further developments in the field of plasmonics. In this regard, MNP-based plasmonic biosensor arrays could be integrated into microfluidic chips for routine point-of-care clinical tests and real-time diagnosis of diseases, as the next generation of biosensors [212]. Also, considering advances in chemical biology, materials science, and synthetic biology, more biosensors will be employed for theranostic (combination of therapeutic and diagnostic) applications via integrating the novel biosensors into carrier agents such as single supramolecular assemblies or NPs (consisting of a trapped prodrug combined with an imaging reagent and a disease specific sensor module), with aim the to detect the endogenous biomarkers of a host organism followed by coupling the readout of the biosensor to a therapeutic modality and consequently releasing the therapeutic agent [213].

Other growing important applications of biosensors include environmental monitoring and detection of potentially toxic contaminants [214] and military-relevant detection of biological warfare agents and terrorist-released threats [215]. Multiplexing describes the simultaneous detection of two or more analytes in a single sample, and this is a recent and growing development [216]. Portability and even wearability [217] of biosensors are other important recent developments [218]. The amazing potential of the modern smartphone has led to a plethora of innovative developments in this area [219]. Finally, it is hoped that MNPs could break through all barriers in bioanalyses, having almost infinite potentials and tremendous scope of functionalities.

Acknowledgments: Support was provided by the National Institute of Allergy and Infectious Diseases (grant/award number R01AI050875).

References

[1] Freire F, Ferraresi C, Jorge AOC, Hamblin MR. Photodynamic therapy of oral Candida infection in a mouse model. *J. Photochem. Photobiol. B Biol*. 2016, 159, 161–168.

[2] Wang Y, Wu X, Chen J, Amin R, Lu M, Bhayana B, Zhao J, Murray CK, Hamblin MR, Hooper DC, Dai T. Antimicrobial blue light inactivation of gram-negative pathogens in biofilms: in vitro and in vivo studies. *J. Infect. Dis.* 2016, 213, 1380–1387.

[3] Yu C, Avci P, Canteenwala T, Chiang LY, Chen BJ, Hamblin MR. Photodynamic therapy with hexa (sulfo-*n*-butyl)[60] fullerene against sarcoma *in vitro* and *in vivo*. *J. Nanosci. Nanotechnol*. 2016, 16, 171–181.

[4] Karimi M, Avci P, Ahi M, Gazori T, Hamblin MR, Naderi-Manesh H. Evaluation of chitosan-tripolyphosphate nanoparticles as a *p*-shRNA delivery vector: formulation, optimization and cellular uptake study. *J. Nanopharm. Drug Deliv*. 2013, 1, 266–278.

[5] Fathi M, Entezami AA, Ebrahimi A, Safa KD. Synthesis of thermosensitive nanohydrogels by crosslinker free method based on *N*-isopropylacrylamide: applicable in the naltrexone sustained release. *Macromol. Res*. 2013, 21, 17–26.
[6] Massoumi B, Abdollahi M, Fathi M, Entezami AA, Hamidi S. Synthesis of novel thermoresponsive micelles by graft copolymerization of *N*-isopropylacrylamide on poly (ε-caprolactone-co-α-bromo-ε-caprolactone) as macroinitiator via ATRP. *J. Polym. Res*. 2013, 20, 18.
[7] Karimi M, Ghasemi A, Sahandi Zangabad P, Rahighi R, Moosavi Basri SM, Mirshekari H, Amiri M, Shafaei Pishabad Z, Aslani A, Bozorgomid M, Ghosh D, Beyzavi A, Vaseghi A, Aref AR, Haghani L, Bahrami S, Hamblin MR. Smart micro/nanoparticles in stimulus-responsive drug/gene delivery systems. *Chem. Soc. Rev*. 2016, 45, 1457–1501.
[8] Karimi M, Eslami M, Sahandi-Zangabad P, Mirab F, Farajisafiloo N, Shafaei Z, Ghosh D, Bozorgomid M, Dashkhaneh F, Hamblin MR. pH-Sensitive stimulus-responsive nanocarriers for targeted delivery of therapeutic agents. *Wiley Interdiscip. Rev. Nanomed. Nanobiotechnol*. 2016, 8, 696–716.
[9] Karimi M, Mirshekari H, Aliakbari M, Sahandi-Zangabad P, Hamblin MR. Smart mesoporous silica nanoparticles for controlled-release drug delivery. *Nanotechnol. Rev*. 2016, 5, 195–207.
[10] Karimi M, Zangabad PS, Ghasemi A, Hamblin MR. *pH-Sensitive Micro/nanocarriers. Smart Internal Stimulus-Responsive Nanocarriers for Drug and Gene Delivery*, Morgan & Claypool Publishers, 2015.
[11] Karimi M, Zare H, Bakhshian Nik A, Yazdani N, Hamrang M, Mohamed E, Sahandi Zangabad P, Moosavi Basri SM, Bakhtiari L, Hamblin MR. Nanotechnology in diagnosis and treatment of coronary artery disease. *Nanomedicine* 2016, 11, 513–530.
[12] Karimi M, Bahrami S, Ravari SB, Zangabad PS, Mirshekari H, Bozorgomid M, Shahreza S, Sori M, Hamblin MR. Albumin nanostructures as advanced drug delivery systems. *Exp. Opin. Drug Deliv*. 2016, 1–15.
[13] de Freitas LF, Hamblin MR. Antibiotic resistance and viral infections. In *Antimicrobial Photodynamic Inactivation and Antitumor Photodynamic Therapy with Fullerenes*. Morgan & Claypool Publishers: San Rafael, CA, 2016.
[14] Karimi M, Sahandi Zangabad P, Ghasemi A, Amiri M, Bahrami M, Malekzad H, Ghahramanzadeh Asl H, Mahdieh Z, Bozorgomid M, Ghasemi A, Rahmani Taji Boyuk MR. Temperature-responsive smart nanocarriers for delivery of therapeutic agents: applications and recent advances. *ACS Appl. Mater. Interfaces*. 2016, 8, 21107–21133.
[15] Bellan LM, Wu D, Langer RS. Current trends in nanobiosensor technology. *Wiley Interdiscip. Rev. Nanomed. Nanobiotechnol*. 2011, 3, 229–246.
[16] Domínguez-Renedo O, Alonso-Lomillo MA, Arcos-Martínez MJ. Determination of metals based on electrochemical biosensors. *Crit. Rev. Environ. Sci. Technol*. 2013, 43, 1042–1073.
[17] Sener G, Uzun L, Denizli A. Colorimetric sensor array based on gold nanoparticles and amino acids for identification of toxic metal ions in water. *ACS Appl. Mater. Interfaces*. 2014, 6, 18395–18400.
[18] Deng H-H, Li G-W, Hong L, Liu A-L, Chen W, Lin X-H, Xia XH. Colorimetric sensor based on dual-functional gold nanoparticles: analyte-recognition and peroxidase-like activity. *Food Chem*. 2014, 147, 257–261.
[19] Sharma R, Ragavan KV, Thakur MS, Raghavarao K. Recent advances in nanoparticle based aptasensors for food contaminants. *Biosens. Bioelectron*. 2015, 74, 612–627.
[20] Terry LA, White SF, Tigwell LJ. The application of biosensors to fresh produce and the wider food industry. *J. Agricult. Food Chem*. 2005, 53, 1309–1316.
[21] Thévenot DR, Toth K, Durst RA, Wilson GS. Electrochemical biosensors: recommended definitions and classification. *Biosens. Bioelectron*. 2001, 16, 121–31.
[22] Wu B, Kuang Y, Zhang X, Chen J. Noble metal nanoparticles/carbon nanotubes nanohybrids: synthesis and applications. *Nano Today*. 2011, 6, 75–90.
[23] Scheller FW, Yarman A, Bachmann T, Hirsch T, Kubick S, Renneberg R, Schumacher S, Wollenberger U, Teller C, Bier FF. *Future of Biosensors: A Personal View*. Biosensors Based on Aptamers and Enzymes: Springer; 2013. p. 1–28.
[24] Vigneshvar S, Sudhakumari C, Senthilkumaran B, Prakash H. Recent advances in biosensor technology for potential applications – an overview. *Front Bioeng Biotechnol*. 2016, 4, 11.
[25] Perumal V, Hashim U. Advances in biosensors: principle, architecture and applications. *J. Appl. Biomed*. 2014, 12, 1–15.
[26] Long F, Zhu A, Shi H. Recent advances in optical biosensors for environmental monitoring and early warning. *Sensors* 2013, 13, 13928–13948.
[27] Turkmen E, Bas SZ, Gulce H, Yildiz S. Glucose biosensor based on immobilization of glucose oxidase in electropolymerized poly (o-phenylenediamine) film on platinum nanoparticles-polyvinylferrocenium modified electrode. *Electrochim. Acta* 2014, 123, 93–102.
[28] Guo X, Liang B, Jian J, Zhang Y, Ye X. Glucose biosensor based on a platinum electrode modified with rhodium nanoparticles and with glucose oxidase immobilized on gold nanoparticles. *Microchim. Acta*. 2014, 181, 519–25.
[29] Sabouri S, Ghourchian H, Shourian M, Boutorabi M. A gold nanoparticle-based immunosensor for the chemiluminescence detection of the hepatitis B surface antigen. *Anal. Method*. 2014, 6, 5059–5066.
[30] Lin J, Zhang H, Zhang S. New bienzymatic strategy for glucose determination by immobilized-gold nanoparticle-enhanced chemiluminescence. *Sci. China Ser. B* 2009, 52, 196–202.
[31] Liu H, Xu S, He Z, Deng A, Zhu J-J. Supersandwich cytosensor for selective and ultrasensitive detection of cancer cells using aptamer-DNA concatamer-quantum dots probes. *Anal. Chem*. 2013, 85, 3385–3392.
[32] Li Y, Schluesener HJ, Xu S. Gold nanoparticle-based biosensors. *Gold Bull*. 2010, 43, 29–41.
[33] Ronkainen NJ, Halsall HB, Heineman WR. Electrochemical biosensors. *Chem. Soc. Rev*. 2010, 39, 1747–1763.
[34] Tian D, Duan C, Wang W, Li N, Zhang H, Cui H, Lu Y. Sandwich-type electrochemiluminescence immunosensor based on *N*-(aminobutyl)-*N*-ethylisoluminol labeling and gold nanoparticle amplification. *Talanta* 2009, 78, 399–404.
[35] Chaichi MJ, Ehsani M. A novel glucose sensor based on immobilization of glucose oxidase on the chitosan-coated Fe_3O_4 nanoparticles and the luminol-H_2O_2-gold nanoparticle

chemiluminescence detection system. *Sensor. Actuat. B* 2016, 223, 713–722.
[36] Zhang M, Yuan R, Chai Y, Chen S, Zhong H, Wang C, Cheng Y. A biosensor for cholesterol based on gold nanoparticles-catalyzed luminol electrogenerated chemiluminescence. *Biosens. Bioelectron.* 2012, 32, 288–292.
[37] Zhong X, Chai YQ, Yuan R. A novel strategy for synthesis of hollow gold nanosphere and its application in electrogenerated chemiluminescence glucose biosensor. *Talanta* 2014, 128, 9–14.
[38] Yan Z, Yang M, Wang Z, Zhang F, Xia J, Shi G, Xia L, Li Y, Xia Y, Xia L. A label-free immunosensor for detecting common acute lymphoblastic leukemia antigen (CD10) based on gold nanoparticles by quartz crystal microbalance. *Sensor. Actuat. B* 2015, 210, 248–253.
[39] Shan W, Pan Y, Fang H, Guo M, Nie Z, Huang Y, Yao S. An aptamer-based quartz crystal microbalance biosensor for sensitive and selective detection of leukemia cells using silver-enhanced gold nanoparticle label. *Talanta* 2014, 126, 130–135.
[40] Zhang J, Sun Y, Wu Q, Gao Y, Zhang H, Bai Y, Song D. Preparation of graphene oxide-based surface plasmon resonance biosensor with Au bipyramid nanoparticles as sensitivity enhancer. *Colloid. Surface B* 2014, 116, 211–218.
[41] Sugawa K, Tahara H, Yamashita A, Otsuki J, Sagara T, Harumoto T, Yanagida S. Refractive index susceptibility of the plasmonic palladium nanoparticle: potential as the third plasmonic sensing material. *ACS Nano* 2015, 9, 1895–904.
[42] Ding L, Bond AM, Zhai J, Zhang J. Utilization of nanoparticle labels for signal amplification in ultrasensitive electrochemical affinity biosensors: a review. *Anal. Chim. Acta* 2013, 797, 1–12.
[43] Dhand C, Das M, Datta M, Malhotra B. Recent advances in polyaniline based biosensors. *Biosens. Bioelectron.* 2011, 26, 2811–2821.
[44] Ghindilis AL, Atanasov P, Wilkins E. Enzyme-catalyzed direct electron transfer: Fundamentals and analytical applications. *Electroanalysis* 1997, 9, 661–674.
[45] Cui J, Adeloju SB, Wu Y. Integration of a highly ordered gold nanowires array with glucose oxidase for ultra-sensitive glucose detection. *Anal. Chim. Acta* 2014, 809, 134–140.
[46] Liu D, Guo Q, Zhang X, Hou H, You T. PdCo alloy nanoparticle-embedded carbon nanofiber for ultrasensitive nonenzymatic detection of hydrogen peroxide and nitrite. *J. Colloid Interf Sci.* 2015, 450, 168–173.
[47] Ravenna Y, Xia L, Gun J, Mikhaylov AA, Medvedev AG, Lev O, Alfonta L. Biocomposite based on reduced graphene oxide film modified with phenothiazone and flavin adenine dinucleotide-dependent glucose dehydrogenase for glucose sensing and biofuel cell applications. *Anal. Chem.* 2015, 87, 9567–9571.
[48] Alves DC, Silva R, Voiry D, Asefa T, Chhowalla M. Copper nanoparticles stabilized by reduced graphene oxide for CO_2 reduction reaction. *Materials for Renewable and Sustainable Energy.* 2015, 4, 1–7.
[49] Xue K, Zhou S, Shi H, Feng X, Xin H, Song W. A novel amperometric glucose biosensor based on ternary gold nanoparticles/polypyrrole/reduced graphene oxide nanocomposite. *Sens Actuators B Chem.* 2014, 203, 412–416.
[50] Hossain MF, Park JY. Amperometric glucose biosensor based on Pt-Pd nanoparticles supported by reduced graphene oxide and integrated with glucose oxidase. *Electroanalysis* 2014, 26, 940–951.
[51] Szeitner Z, András J, Gyurcsányi RE, Mészáros T. Is less more? Lessons from aptamer selection strategies. *J. Pharm. Biomed. Anal.* 2014, 101, 58–65.
[52] Wang W, Xie Y, Xia C, Du H, Tian F. Titanium dioxide nanotube arrays modified with a nanocomposite of silver nanoparticles and reduced graphene oxide for electrochemical sensing. *Microchim. Acta* 2014, 181, 1325–1331.
[53] Zhou X, Dai X, Li J, Long Y, Li W, Tu Y. A sensitive glucose biosensor based on Ag@ C core-shell matrix. *Mater. Sci. Eng.* 2015, 49, 579–587.
[54] Ghosh Chaudhuri R, Paria S. Core/shell nanoparticles: classes, properties, synthesis mechanisms, characterization, and applications. *Chem. Rev.* 2011, 112, 2373–2433.
[55] Mani V, Dinesh B, Chen S-M, Saraswathi R. Direct electrochemistry of myoglobin at reduced graphene oxide-multiwalled carbon nanotubes-platinum nanoparticles nanocomposite and biosensing towards hydrogen peroxide and nitrite. *Biosens. Bioelectron.* 2014, 53, 420–427.
[56] Mir TA, Akhtar MH, Gurudatt NG, Kim J-I, Choi CS, Shim Y-B. An amperometric nanobiosensor for the selective detection of K+-induced dopamine released from living cells. *Biosens. Bioelectron.* 2015, 68, 421–428.
[57] Nesakumar N, Thandavan K, Sethuraman S, Krishnan UM, Rayappan JBB. An electrochemical biosensor with nano-interface for lactate detection based on lactate dehydrogenase immobilized on zinc oxide nanorods. *J. Colloid Interf. Sci.* 2014, 414, 90–96.
[58] Sardesai NP, Ganesana M, Karimi A, Leiter JC, Andreescu S. Platinum-doped ceria based biosensor for in vitro and in vivo monitoring of lactate during hypoxia. *Anal. Chem.* 2015, 87, 2996–3003.
[59] Zhao Y, Fang X, Gu Y, Yan X, Kang Z, Zheng X, Lin P, Zhao L, Zhang Y. Gold nanoparticles coated zinc oxide nanorods as the matrix for enhanced L-lactate sensing. *Colloid. Surface B* 2015, 126, 476–480.
[60] Loaiza OA, Lamas-Ardisana PJ, Añorga L, Jubete E, Ruiz V, Borghei M, Cabañero G, Grande HJ. Graphitized carbon nanofiber-Pt nanoparticle hybrids as sensitive tool for preparation of screen printing biosensors. Detection of lactate in wines and ciders. *Bioelectrochemistry* 2015, 101, 58–65.
[61] Wang L, Wen W, Xiong H, Zhang X, Gu H, Wang S. A novel amperometric biosensor for superoxide anion based on superoxide dismutase immobilized on gold nanoparticle-chitosan-ionic liquid biocomposite film. *Anal Chim. Acta* 2013, 758, 66–71.
[62] Warwick C, Guerreiro A, Soares A. Sensing and analysis of soluble phosphates in environmental samples: a review. *Biosens. Bioelectron.* 2013, 41, 1–11.
[63] Huang K-J, Liu Y-J, Wang H-B, Gan T, Liu Y-M, Wang L-L. Signal amplification for electrochemical DNA biosensor based on two-dimensional graphene analogue tungsten sulfide–graphene composites and gold nanoparticles. *Sensor. Actuator. B* 2014, 191, 828–836.
[64] Ekram H, Galal A, Atta NF. Electrochemistry of glucose at gold nanoparticles modified graphite/SrPdO 3 electrode – towards a novel non-enzymatic glucose sensor. *J. Electroanal. Chem.* 2015, 749, 42–52.
[65] Yuan M, Liu A, Zhao M, Dong W, Zhao T, Wang J, Tang W. Bimetallic PdCu nanoparticle decorated three-dimensional graphene hydrogel for non-enzymatic amperometric glucose sensor. *Sensor. Actuator. B* 2014, 190, 707–714.

[66] Chang G, Shu H, Ji K, Oyama M, Liu X, He Y. Gold nanoparticles directly modified glassy carbon electrode for non-enzymatic detection of glucose. *Appl. Surf. Sci.* 2014, 288, 524–529.
[67] Zhang Z, Liu S, Shi Y, Zhang Y, Peacock D, Yan F, Wang P, He L, Feng X, Fang S. Label-free aptamer biosensor for thrombin detection on a nanocomposite of graphene and plasma polymerized allylamine. *J. Mater. Chem. B* 2014, 2, 1530–1538.
[68] Wang Y, Chen J, Zhou C, Zhou L, Kong Y, Long H, Zhong S. A novel self-cleaning, non-enzymatic glucose sensor working under a very low applied potential based on a Pt nanoparticle-decorated TiO 2 nanotube array electrode. *Electrochim. Acta* 2014, 115, 269–276.
[69] Maji SK, Sreejith S, Mandal AK, Ma X, Zhao Y. Immobilizing gold nanoparticles in mesoporous silica covered reduced graphene oxide: a hybrid material for cancer cell detection through hydrogen peroxide sensing. *ACS Appl. Mater. Interfaces* 2014, 6, 13648–13656.
[70] Toccafondi C, Thorat S, La Rocca R, Scarpellini A, Salerno M, Dante S, Das G. Multifunctional substrates of thin porous alumina for cell biosensors. *J. Mater. Sci. Mater. Med.* 2014, 25, 2411–2420.
[71] Jiang Z, Yang T, Liu M, Hu Y, Wang J. An aptamer-based biosensor for sensitive thrombin detection with phthalocyanine@ SiO 2 mesoporous nanoparticles. *Biosens. Bioelectron.* 2014, 53, 340–345.
[72] Dhara K, Stanley J, Ramachandran T, Nair BG. Pt-CuO nanoparticles decorated reduced graphene oxide for the fabrication of highly sensitive non-enzymatic disposable glucose sensor. *Sensor. Actuator. B* 2014, 195, 197–205.
[73] Yin G, Xing L, Ma X-J, Wan J. Non-enzymatic hydrogen peroxide sensor based on a nanoporous gold electrode modified with platinum nanoparticles. *Chem. Pap.* 2014, 68, 435–441.
[74] Gougis M, Tabet-Aoul A, Ma D, Mohamedi M. Laser synthesis and tailor-design of nanosized gold onto carbon nanotubes for non-enzymatic electrochemical glucose sensor. *Sensor. Actuator. B* 2014, 193, 363–369.
[75] Ensafi AA, Abarghoui MM, Rezaei B. A new non-enzymatic glucose sensor based on copper/porous silicon nanocomposite. *Electrochim. Acta* 2014, 123, 219–226.
[76] Zhou Z, Li L, Yang Y, Xu X, Huang Y. Tumor targeting by pH-sensitive, biodegradable, cross-linked N-(2-hydroxypropyl) methacrylamide copolymer micelles. *Biomaterials* 2014, 35, 6622–6635.
[77] Ojeda I, Moreno-Guzmán M, González-Cortés A, Yáñez-Sedeño P, Pingarrón JM. A disposable electrochemical immunosensor for the determination of leptin in serum and breast milk. *Analyst* 2013, 138, 4284–91.
[78] Cork J, Jones RM, Sawyer J. Low cost, disposable biosensors allow detection of antibodies with results equivalent to ELISA in 15 min. *J. Immunol. Methods.* 2013, 387, 140–146.
[79] Jeong B, Akter R, Han OH, Rhee CK, Rahman MA. Increased electrocatalyzed performance through dendrimer-encapsulated gold nanoparticles and carbon nanotube-assisted multiple bienzymatic labels: highly sensitive electrochemical immunosensor for protein detection. *Anal. Chem.* 2013, 85, 1784–1791.
[80] Han K, Liang Z, Zhou N. Design strategies for aptamer-based biosensors. *Sensors* 2010, 10, 4541–4557.
[81] Famulok M, Mayer G. Aptamers and SELEX in chemistry & biology. *Chem. Biol.* 2014, 21, 1055–1058.
[82] Wang Z, Liu N, Ma Z. Platinum porous nanoparticles hybrid with metal ions as probes for simultaneous detection of multiplex cancer biomarkers. *Biosens. Bioelectron.* 2014, 53, 324–329.
[83] Liu Y, Xu L-P, Wang S, Yang W, Wen Y, Zhang X. An ultrasensitive electrochemical immunosensor for apolipoprotein E4 based on fractal nanostructures and enzyme amplification. *Biosens. Bioelectron.* 2015, 71, 396–400.
[84] Lin D, Wu J, Ju H, Yan F. Nanogold/mesoporous carbon foam-mediated silver enhancement for graphene-enhanced electrochemical immunosensing of carcinoembryonic antigen. *Biosens. Bioelectron.* 2014, 52, 153–158.
[85] Wang Y, Zhang Y, Su Y, Li F, Ma H, Li H, Du B, Wei Q. Ultrasensitive non-mediator electrochemical immunosensors using Au/Ag/Au core/double shell nanoparticles as enzyme-mimetic labels. *Talanta* 2014, 124, 60–66.
[86] Xu T, Jia X, Chen X, Ma Z. Simultaneous electrochemical detection of multiple tumor markers using metal ions tagged immunocolloidal gold. *Biosens. Bioelectron.* 2014, 56, 174–179.
[87] Yang C, Wang Q, Xiang Y, Yuan R, Chai Y. Target-induced strand release and thionine-decorated gold nanoparticle amplification labels for sensitive electrochemical aptamer-based sensing of small molecules. *Sensor. Actuator. B* 2014, 197, 149–154.
[88] Odenthal KJ, Gooding JJ. An introduction to electrochemical DNA biosensors. *Analyst* 2007, 132, 603–610.
[89] Wang L, Hua E, Liang M, Ma C, Liu Z, Sheng S, Liu M, Xie G, Feng W. Graphene sheets, polyaniline and AuNPs based DNA sensor for electrochemical determination of BCR/ABL fusion gene with functional hairpin probe. *Biosens. Bioelectron.* 2014, 51, 201–207.
[90] Wang P, Xu G, Qin L, Xu Y, Li Y, Li R. Cell-based biosensors and its application in biomedicine. *Sensor. Actuator. B* 2005, 108, 576–584.
[91] Hafner F. Cytosensor® Microphysiometer: technology and recent applications. *Biosens. Bioelectron.* 2000, 15, 149–158.
[92] Eklund SE, Cliffel DE, Kozlov E, Prokop A, Wikswo J, Baudenbacher F. Modification of the Cytosensor™ microphysiometer to simultaneously measure extracellular acidification and oxygen consumption rates. *Anal. Chim. Acta* 2003, 496, 93–101.
[93] Hun X, Liu F, Mei Z, Ma L, Wang Z, Luo X. Signal amplified strategy based on target-induced strand release coupling cleavage of nicking endonuclease for the ultrasensitive detection of ochratoxin A. *Biosens. Bioelectron.* 2013, 39, 145–151.
[94] Ding L, Ju H. Biofunctionalization of nanoparticles for cytosensing and cell surface carbohydrate assay. *J. Mater. Chem.* 2011, 21, 18154–18173.
[95] Shao M-L, Bai H-J, Gou H-L, Xu J-J, Chen H-Y. Cytosensing and evaluation of cell surface glycoprotein based on a biocompatible poly (diallydimethylammonium) doped poly (dimethylsiloxane) film. *Langmuir* 2009, 25, 3089–3095.
[96] Zhang J-J, Cheng F-F, Zheng T-T, Zhu J-J. Design and implementation of electrochemical cytosensor for evaluation of cell surface carbohydrate and glycoprotein. *Anal. Chem.* 2010, 82, 3547–3555.
[97] Cai H-H, Pi J, Lin X, Li B, Li A, Yang P-H, Cai J. Gold nanoprobes-based resonance Rayleigh scattering assay platform: sensitive cytosensing of breast cancer cells and facile monitoring of folate receptor expression. *Biosens. Bioelectron.* 2015;74:165–9.

[98] Xu S, Liu J, Wang T, Li H, Miao Y, Liu Y, Wang J, Wang E. A simple and rapid electrochemical strategy for non-invasive, sensitive and specific detection of cancerous cell. *Talanta* 2013, 104, 122–127.
[99] Hu C, Yang D-P, Wang Z, Yu L, Zhang J, Jia N. Improved EIS performance of an electrochemical cytosensor using three-dimensional architecture Au@ BSA as sensing layer. *Anal. Chem.* 2013, 85, 5200–5206.
[100] Sun D, Lu J, Zhong Y, Yu Y, Wang Y, Zhang B, Chen Z. Sensitive electrochemical aptamer cytosensor for highly specific detection of cancer cells based on the hybrid nanoelectrocatalysts and enzyme for signal amplification. *Biosens. Bioelectron.* 2016, 75, 301–307.
[101] Tepeli Y, Demir B, Timur S, Anik U. An electrochemical cytosensor based on a PAMAM modified glassy carbon paste electrode. *RSC Adv.* 2015, 5, 53973–53978.
[102] Zhang S, Zhang L, Zhang X, Yang P, Cai J. An efficient nanomaterial-based electrochemical biosensor for sensitive recognition of drug-resistant leukemia cells. *Analyst* 2014, 139, 3629–3635.
[103] Sun D, Lu J, Chen Z, Yu Y, Mo M. A repeatable assembling and disassembling electrochemical aptamer cytosensor for ultrasensitive and highly selective detection of human liver cancer cells. *Anal. Chim. Acta* 2015, 885, 166–173.
[104] Zheng T, Fu J-J, Hu L, Qiu F, Hu M, Zhu J-J, Hua Z-C, Wang H. Nanoarchitectured electrochemical cytosensors for selective detection of leukemia cells and quantitative evaluation of death receptor expression on cell surfaces. *Anal. Chem.* 2013, 85, 5609–5616.
[105] Chen Z, Liu Y, Wang Y, Zhao X, Li J. Dynamic evaluation of cell surface *N*-glycan expression via an electrogenerated chemiluminescence biosensor based on concanavalin A-integrating gold-nanoparticle-modified Ru(bpy)32+-doped silica nanoprobe. *Anal. Chem.* 2013, 85, 4431–4438.
[106] Wang H, Cai H-H, Zhang L, Cai J, Yang P-H, Chen ZW. A novel gold nanoparticle-doped polyaniline nanofibers-based cytosensor confers simple and efficient evaluation of T-cell activation. *Biosens. Bioelectron.* 2013, 50, 167–173.
[107] Tang Y, Zhang S, Wen Q, Huang H, Yang P. A sensitive electrochemiluminescence cytosensor for quantitative evaluation of epidermal growth factor receptor expressed on cell surfaces. *Anal. Chim. Acta* 2015, 881, 148–154.
[108] Lu W, Wang H-Y, Wang M, Wang Y, Tao L, Qian W. Au nanoparticle decorated resin microspheres: synthesis and application in electrochemical cytosensors for sensitive and selective detection of lung cancer A549 cells. *RSC Adv.* 2015, 5, 24615–24624.
[109] Chandrasekaran A, Deng K, Koh C-Y, Takasuka T, Bergeman LF, Fox BG, Adams PD, Singh AK. A universal flow cytometry assay for screening carbohydrate-active enzymes using glycan microspheres. *Chem Commun.* 2013, 49, 5441–5443.
[110] Guo X. Surface plasmon resonance based biosensor technique: a review. *J. Biophotonics* 2012, 5, 483–501.
[111] Haes AJ, Van Duyne RP. A unified view of propagating and localized surface plasmon resonance biosensors. *Anal. Bioanal. Chem.* 2004, 379, 920–930.
[112] Szunerits S, Boukherroub R. Sensing using localised surface plasmon resonance sensors. *Chem. Commun.* 2012, 48, 8999–9010.
[113] Jain PK, Huang X, El-Sayed IH, El-Sayed MA. Noble metals on the nanoscale: optical and photothermal properties and some applications in imaging, sensing, biology, and medicine. *Accounts Chem. Res.* 2008, 41, 1578–1586.
[114] Soares L, Csáki A, Jatschka J, Fritzsche W, Flores O, Franco R, Pereira E. Localized surface plasmon resonance (LSPR) biosensing using gold nanotriangles: detection of DNA hybridization events at room temperature. *Analyst* 2014, 139, 4964–4973.
[115] Brandon MP, Ledwith DM, Kelly JM. Preparation of saline-stable, silica-coated triangular silver nanoplates of use for optical sensing. *J. Colloid Interf. Sci.* 2014, 415, 77–84.
[116] Zhao Q, Duan R, Yuan J, Quan Y, Yang H, Xi M. A reusable localized surface plasmon resonance biosensor for quantitative detection of serum squamous cell carcinoma antigen in cervical cancer patients based on silver nanoparticles array. *Int. J. Nanomedicine* 2014, 9, 1097–1104.
[117] Yang X, Yu Y, Gao Z. A Highly sensitive plasmonic DNA assay based on triangular silver nanoprism etching. *ACS Nano.* 2014, 8, 4902–4907.
[118] Jung B, Frey W. Fabrication and localized surface plasmon properties of triangular gold nanowell arrays in a glass substrate. *J. Nanosci. Nanotechnol.* 2015, 15, 688–692.
[119] Kegel LL, Boyne D, Booksh KS. Sensing with Prism-based near-infrared surface plasmon resonance spectroscopy on nanohole array platforms. *Anal. Chem.* 2014, 86, 3355–3364.
[120] Barik A, Otto LM, Yoo D, Jose J, Johnson TW, Oh S-H. Dielectrophoresis-enhanced plasmonic sensing with gold nanohole arrays. *Nano Lett.* 2014, 14, 2006–2012.
[121] Lepinay S, Staff A, Ianoul A, Albert J. Improved detection limits of protein optical fiber biosensors coated with gold nanoparticles. *Biosens. Bioelectron.* 2014, 52, 337–344.
[122] Zagorodko O, Spadavecchia J, Serrano AY, Larroulet I, Pesquera A, Zurutuza A, Boukherroub R, Szunerits S. Highly sensitive detection of DNA hybridization on commercialized graphene-coated surface plasmon resonance interfaces. *Anal. Chem.* 2014, 86, 11211–11216.
[123] Duan N, Wu S, Dai S, Miao T, Chen J, Wang Z. Simultaneous detection of pathogenic bacteria using an aptamer based biosensor and dual fluorescence resonance energy transfer from quantum dots to carbon nanoparticles. *Microchim. Acta.* 2014, 182, 917–923.
[124] Yao G-H, Liang R-P, Huang C-F, Zhang L, Qiu J-D. Enzyme-free surface plasmon resonance aptasensor for amplified detection of adenosine via target-triggering strand displacement cycle and Au nanoparticles. *Anal. Chim. Acta* 2015, 871, 28–34.
[125] Baek SH, Wark AW, Lee HJ. Dual nanoparticle amplified surface plasmon resonance detection of thrombin at subattomolar concentrations. *Anal. Chem.* 2014, 86, 9824–9829.
[126] Chen S, Gao H, Shen W, Lu C, Yuan Q. Colorimetric detection of cysteine using noncrosslinking aggregation of fluorosurfactant-capped silver nanoparticles. *Sensor. Actuator. B* 2014, 190, 673–678.
[127] Sciacca B, Monro TM. Dip biosensor based on localized surface plasmon resonance at the tip of an optical fiber. *Langmuir* 2014, 30, 946–954.

[128] Jiao H, Chen J, Li W, Wang F, Zhou H, Li Y, Yu C. Nucleic acid-regulated perylene probe-induced gold nanoparticle aggregation: a new strategy for colorimetric sensing of alkaline phosphatase activity and inhibitor screening. *ACS Appl. Mater. Interfaces* 2014, 6, 1979–1985.
[129] Bharadwaj R, Mukherji S. Gold nanoparticle coated U-bend fibre optic probe for localized surface plasmon resonance based detection of explosive vapours. *Sensor Actuator. B* 2014, 192, 804–811.
[130] Norek M, Włodarski M, Matysik P. UV plasmonic-based sensing properties of aluminum nanoconcave arrays. *Curr. Appl. Phys.* 2014, 14, 1514–1520.
[131] Kumeria T, Rahman MM, Santos A, Ferré-Borrull J, Marsal LF, Losic D. Structural and optical nanoengineering of nanoporous anodic alumina rugate filters for real-time and label-free biosensing applications. *Anal. Chem.* 2014, 86, 1837–1844.
[132] Park J-H, Byun J-Y, Mun H, Shim W-B, Shin Y-B, Li T, Kim MG. A regeneratable, label-free, localized surface plasmon resonance (LSPR) aptasensor for the detection of ochratoxin A. *Biosens. Bioelectron.* 2014, 59, 321–327.
[133] Chen F, Fei W, Sun L, Li Q, Di J, Wu Y. Direct growth of coupled gold nanoparticles on indium tin oxide substrate and construction of biosensor based on localized surface plasmon resonance. *Sensor. Actuator. B* 2014, 191, 337–343.
[134] da Silva CTP, Monteiro JP, Radovanovic E, Girotto EM. Unprecedented high plasmonic sensitivity of substrates based on gold nanoparticles. *Sensor. Actuator. B* 2014, 191, 152–157.
[135] Ma W, Xu L, Wang L, Kuang H, Xu C. Orientational nanoparticle assemblies and biosensors. *Biosens. Bioelectron.* 2016, 79, 220–236.
[136] Dong J, Zheng H, Zhang Z, Gao W, Liu J, He E. Surface enhanced fluorescence by plasmonic nanostructures. Reviews in Plasmonics 2015: Springer, 2016. p. 387–415.
[137] Schäferling M. Fluorescence-based biosensors. Encyclopedia of Analytical Chemistry: John Wiley & Sons, Ltd, 2006.
[138] Jain PK, Huang X, El-Sayed IH, El-Sayed MA. Review of some interesting surface plasmon resonance-enhanced properties of noble metal nanoparticles and their applications to biosystems. *Plasmonics* 2007, 2, 107–118.
[139] Aslan K, Gryczynski I, Malicka J, Matveeva E, Lakowicz JR, Geddes CD. Metal-enhanced fluorescence: an emerging tool in biotechnology. *Curr. Opin. Biotechnol.* 2005, 16, 55–62.
[140] Swierczewska M, Lee S, Chen X. The design and application of fluorophore-gold nanoparticle activatable probes. *Phys. Chem. Chem. Phys.* 2011, 13, 9929–9941.
[141] Chinen AB, Guan CM, Ferrer JR, Barnaby SN, Merkel TJ, Mirkin CA. Nanoparticle probes for the detection of cancer biomarkers, cells, and tissues by fluorescence. *Chem. Rev.* 2015, 115, 10530–10574.
[142] Shamsipur M, Memari Z, Ganjali MR, Norouzi P, Faridbod F. Highly sensitive gold nanoparticles-based optical sensing of DNA hybridization using bis(8-hydroxyquinoline-5-solphonate)cerium(III) chloride as a novel fluorescence probe. *J. Pharm. Biomed. Anal.* 2016, 118, 356–362.
[143] Huang D, Niu C, Wang X, Lv X, Zeng G. "Turn-On" fluorescent sensor for Hg2+ based on single-stranded DNA functionalized Mn: CdS/ZnS quantum dots and gold nanoparticles by time-gated mode. *Anal. Chem.* 2013, 85, 1164–1170.
[144] Zhu J, Wang J-F, Li J-J, Zhao J-W. Tuning the fluorescence quenching properties of plasmonic Ag-coated-au triangular nanoplates: application in ultrasensitive detection of CEA. *Plasmonics* 2015, 11, 565–572.
[145] Jeong HY, Baek SH, Chang SJ, Cheon SA, Park TJ. Robust fluorescence sensing platform for detection of CD44 cells based on graphene oxide/gold nanoparticles. *Colloid. Surface B* 2015, 135, 309–315.
[146] Lakowicz JR. Radiative decay engineering 5: metal-enhanced fluorescence and plasmon emission. *Anal. Biochem.* 2005, 337, 171–194.
[147] Tang Y, Yang Q, Wu T, Liu L, Ding Y, Yu B. Fluorescence enhancement of cadmium selenide quantum dots assembled on silver nanoparticles and its application to glucose detection. *Langmuir* 2014, 30, 6324–6330.
[148] Xu YK, Hwang S, Kim S, Chen JY. Two orders of magnitude fluorescence enhancement of aluminum phthalocyanines by gold nanocubes: a remarkable improvement for cancer cell imaging and detection. *ACS Appl. Mater. Interfaces* 2014, 6, 5619–5628.
[149] Seitz WR. Immunoassay labels based on chemiluminescence and bioluminescence. Clin. Biochem. 1984, 17, 120–125.
[150] Zhang Z-F, Cui H, Lai C-Z, Liu L-J. Gold nanoparticle-catalyzed luminol chemiluminescence and its analytical applications. *Anal. Chem.* 2005, 77, 3324–339.
[151] Fan A, Lau C, Lu J. Magnetic bead-based chemiluminescent metal immunoassay with a colloidal gold label. *Anal Chem.* 2005, 77, 3238–3242.
[152] Roda A, Pasini P, Mirasoli M, Michelini E, Guardigli M. Biotechnological applications of bioluminescence and chemiluminescence. *Trends Biotechnol.* 2004, 22, 295–303.
[153] Li Y, Qi H, Peng Y, Yang J, Zhang C. Electrogenerated chemiluminescence aptamer-based biosensor for the determination of cocaine. *Electrochem. Commun.* 2007, 9, 2571–2575.
[154] Miao W. Electrogenerated chemiluminescence and its biorelated applications. *Chem. Rev.* 2008, 108, 2506–2553.
[155] Fähnrich KA, Pravda M, Guilbault GG. Recent applications of electrogenerated chemiluminescence in chemical analysis. *Talanta* 2001, 54, 531–559.
[156] Bi S, Yan Y, Yang X, Zhang S. Gold nanolabels for new enhanced chemiluminescence immunoassay of alpha-fetoprotein based on magnetic beads. *Chemistry* 2009, 15, 4704–4709.
[157] Yang Z, Cao Y, Li J, Wang J, Du D, Hu X, Lin Y. A new label-free strategy for a highly efficient chemiluminescence immunoassay. *Chem. Commun. (Camb).* 2015, 51, 14443–14446.
[158] Chen L, Zeng X, Si P, Chen Y, Chi Y, Kim DH, Chen G. Gold nanoparticle-graphite-like C3N4 nanosheet nanohybrids used for electrochemiluminescent immunosensor. *Anal. Chem.* 2014, 86, 4188–4195.
[159] Wang H, He Y, Chai Y, Yuan R. A super intramolecular self-enhanced electrochemiluminescence immunosensor based on polymer chains grafted on palladium nanocages. *Nanoscale* 2014, 6, 10316–10322.
[160] Xiong C, Wang H, Yuan Y, Chai Y, Yuan R. A novel solid-state Ru(bpy)3(2+) electrochemiluminescence immunosensor based on poly(ethylenimine) and polyamidoamine dendrimers as co-reactants. *Talanta* 2015, 131, 192–197.
[161] Moyano DF, Saha K, Prakash G, Yan B, Kong H, Yazdani M, Rotello VM. Fabrication of corona-free nanoparticles with tunable hydrophobicity. *ACS Nano* 2014, 8, 6748–6755.
[162] Lan D, Li B, Zhang Z. Chemiluminescence flow biosensor for glucose based on gold nanoparticle-enhanced activities of

glucose oxidase and horseradish peroxidase. *Biosens. Bioelectron.* 2008, 24, 940–944.
[163] Zargoosh K, Chaichi MJ, Shamsipur M, Hossienkhani S, Asghari S, Qandalee M. Highly sensitive glucose biosensor based on the effective immobilization of glucose oxidase/carbon-nanotube and gold nanoparticle in nafion film and peroxyoxalate chemiluminescence reaction of a new fluorophore. *Talanta* 2012, 93, 37–43.
[164] Zhang L, Xu Z, Sun X, Dong S. A novel alcohol dehydrogenase biosensor based on solid-state electrogenerated chemiluminescence by assembling dehydrogenase to Ru (bpy) 3 2+–Au nanoparticles aggregates. *Biosens. Bioelectron.* 2007, 22, 1097–1100.
[165] Chen H, Tan X, Zhang J, Lu Q, Ou X, Ruo Y, Chen S. An electrogenerated chemiluminescent biosensor based on a g-C3N4-hemin nanocomposite and hollow gold nanoparticles for the detection of lactate. *RSC Adv.* 2014, 4, 61759–6166.
[166] Lou J, Liu S, Tu W, Dai Z. Graphene quantums dots combined with endonuclease cleavage and bidentate chelation for highly sensitive electrochemiluminescent DNA biosensing. *Anal. Chem.* 2015, 87, 1145–1151.
[167] Zhang S, Zhong H, Ding C. Ultrasensitive flow injection chemiluminescence detection of DNA hybridization using signal DNA probe modified with Au and CuS nanoparticles. *Anal. Chem.* 2008, 80, 7206–7212.
[168] Wang X, Ge L, Yu Y, Dong S, Li F. Highly sensitive electrogenerated chemiluminescence biosensor based on hybridization chain reaction and amplification of gold nanoparticles for DNA detection. *Sensor. Actuator. B* 2015, 220, 942–98.
[169] Li Z-P, Wang Y-C, Liu C-H, Li Y-K. Development of chemiluminescence detection of gold nanoparticles in biological conjugates for immunoassay. *Anal. Chim. Acta* 2005, 551, 85–91.
[170] Wang P, Song Y, Zhao Y, Fan A. Hydroxylamine amplified gold nanoparticle-based aptameric system for the highly selective and sensitive detection of platelet-derived growth factor. *Talanta* 2013, 103, 392–397.
[171] Yao L-Y, Yu X-Q, Zhao Y-J, Fan A-P. An aptamer-based chemiluminescence method for ultrasensitive detection of platelet-derived growth factor by cascade amplification combining rolling circle amplification with hydroxylamine-enlarged gold nanoparticles. *Anal. Methods* 2015, 7, 8786–92.
[172] Gill R, Polsky R, Willner I. Pt nanoparticles functionalized with nucleic acid act as catalytic labels for the chemiluminescent detection of DNA and proteins. *Small* 2006, 2, 1037–1041.
[173] Hong LR, Chai YQ, Zhao M, Liao N, Yuan R, Zhuo Y. Highly efficient electrogenerated chemiluminescence quenching of PEI enhanced Ru(bpy)(3)(2)(+) nanocomposite by hemin and Au@CeO(2) nanoparticles. *Biosens. Bioelectron.* 2015, 63, 392–398.
[174] Ding C, Wei S, Liu H. Electrochemiluminescent determination of cancer cells based on aptamers, nanoparticles, and magnetic beads. *Chem. Eur. J.* 2012, 18, 7263–7268.
[175] Ge L, Su M, Gao C, Tao X, Ge S. Application of Au cage/Ru (bpy) 3 2+ nanostructures for the electrochemiluminescence detection of K562 cancer cells based on aptamer. *Sensor. Actuator. B* 2015, 214, 144–151.
[176] Qiu Y, Wen Q, Zhang L, Yang P. Label-free and dynamic evaluation of cell-surface epidermal growth factor receptor expression via an electrochemiluminescence cytosensor. *Talanta* 2016, 150, 286–295.
[177] Liang W, Zhuo Y, Xiong C, Zheng Y, Chai Y, Yuan R. Ultrasensitive cytosensor based on self-enhanced electrochemiluminescent ruthenium-silica composite nanoparticles for efficient drug screening with cell apoptosis monitoring. *Anal. Chem.* 2015, 87, 12363–12371.
[178] Chen D, Zhang H, Li X, Li J. Biofunctional titania nanotubes for visible-light-activated photoelectrochemical biosensing. *Anal. Chem.* 2010, 82, 2253–2261.
[179] Zhang X, Guo Y, Liu M, Zhang S. Photoelectrochemically active species and photoelectrochemical biosensors. *RSC Adv.* 2013, 3, 2846–2857.
[180] Voccia D, Palchetti I. Photoelectrochemical biosensors for nucleic acid detection. *J. Nanosci. Nanotechno.* 2015, 15, 3320–3332.
[181] Devadoss A, Sudhagar P, Terashima C, Nakata K, Fujishima A. Photoelectrochemical biosensors: new insights into promising photoelectrodes and signal amplification strategies. *J. Photochem. Photobiol. A Chem.* 2015, 24, 43–63.
[182] Tian Y, Tatsuma T. Mechanisms and applications of plasmon-induced charge separation at TiO2 films loaded with gold nanoparticles. *J. Am. Chem. Soc.* 2005, 127, 7632–7637.
[183] Da P, Li W, Lin X, Wang Y, Tang J, Zheng G. Surface plasmon resonance enhanced real-time photoelectrochemical protein sensing by gold nanoparticle-decorated TiO2 nanowires. *Anal. Chem.* 2014, 86, 6633–6639.
[184] Zhao WW, Xu JJ, Chen HY. Photoelectrochemical bioanalysis: the state of the art. *Chem. Soc. Rev.* 2015;44, 729–741.
[185] Liu S, Cao H, Wang Z, Tu W, Dai Z. Label-free photoelectrochemical cytosensing via resonance energy transfer using gold nanoparticle-enhanced carbon dots. *Chem. Commun.* 2015, 51, 14259–14262.
[186] Zhao WW, Yu PP, Shan Y, Wang J, Xu JJ, Chen HY. Exciton-plasmon interactions between CdS quantum dots and Ag nanoparticles in photoelectrochemical system and its biosensing application. *Anal. Chem.* 2012, 84, 5892–5897.
[187] Hu Y, Xue Z, He H, Ai R, Liu X, Lu X. Photoelectrochemical sensing for hydroquinone based on porphyrin-functionalized Au nanoparticles on graphene. *Biosens. Bioelectron.* 2013, 47, 45–49.
[188] Liu X, Zhang J, Liu S, Zhang Q, Liu X, Wong DK. Gold nanoparticle encapsulated-tubular TiO2 nanocluster as a scaffold for development of thiolated enzyme biosensors. *Anal. Chem.* 2013, 85, 4350–4356.
[189] Zhang X, Xu Y, Yang Y, Jin X, Ye S, Zhang S, Jiang L. A new signal-on photoelectrochemical biosensor based on a graphene/quantum-dot nanocomposite amplified by the dual-quenched effect of bipyridinium relay and AuNPs. *Chemistry* 2012, 18, 16411–16418.
[190] Zhao M, Fan G-C, Chen J-J, Shi J-J, Zhu J-J. Highly sensitive and selective photoelectrochemical biosensor for Hg2+ Detection based on dual signal amplification by exciton energy transfer coupled with sensitization effect. *Anal. Chem.* 2015, 87, 12340–12347.
[191] Chen S, Hai X, Chen X-W, Wang J-H. In situ growth of silver nanoparticles on graphene quantum dots for ultrasensitive colorimetric detection of H2O2 and glucose. *Anal. Chem.* 2014, 86, 6689–6694.
[192] Cao K, Jiang X, Yan S, Zhang L, Wu W. Phenylboronic acid modified silver nanoparticles for colorimetric dynamic analysis of glucose. *Biosens. Bioelectron.* 2014, 52, 188–195.
[193] Zhang L-N, Deng H-H, Lin F-L, Xu X-W, Weng S-H, Liu A-L, Lin XH, Xia XH, Chen W. In situ growth of porous platinum

nanoparticles on graphene oxide for colorimetric detection of cancer cells. *Anal. Chem.* 2014, 86, 2711–2718.
[194] Zhou C-H, Zhao J-Y, Pang D-W, Zhang Z-L. Enzyme-induced metallization as a signal amplification strategy for highly sensitive colorimetric detection of avian influenza virus particles. *Anal. Chem.* 2014, 86, 2752–2759.
[195] Zhou Y, Dong H, Liu L, Li M, Xiao K, Xu M. Selective and sensitive colorimetric sensor of mercury (II) based on gold nanoparticles and 4-mercaptophenylboronic acid. *Sensor. Actuator. B* 2014, 196, 106–111.
[196] Kumar VV, Anthony SP. Silver nanoparticles based selective colorimetric sensor for Cd 2+, Hg 2+ and Pb 2+ ions: tuning sensitivity and selectivity using co-stabilizing agents. *Sensor. Actuator. B* 2014, 191, 31–36.
[197] Maity D, Gupta R, Gunupuru R, Srivastava DN, Paul P. Calix [4] arene functionalized gold nanoparticles: application in colorimetric and electrochemical sensing of cobalt ion in organic and aqueous medium. *Sensor. Actuator. B* 2014, 191, 757–764.
[198] Deng H-H, Wu C-L, Liu A-L, Li G-W, Chen W, Lin X-H. Colorimetric sensor for thiocyanate based on anti-aggregation of citrate-capped gold nanoparticles. *Sensor. Actuator. B* 2014, 191, 479–484.
[199] Chen G-H, Chen W-Y, Yen Y-C, Wang C-W, Chang H-T, Chen C-F. Detection of mercury (II) ions using colorimetric gold nanoparticles on paper-based analytical devices. *Anal. Chem.* 2014, 86, 6843–6849.
[200] Guan H, Liu X, Wang W, Liang J. Direct colorimetric biosensing of mercury (II) ion based on aggregation of poly-(γ-glutamic acid)-functionalized gold nanoparticles. *Spectrochim. Acta A* 2014, 121, 527–532.
[201] Duan J, Yin H, Wei R, Wang W. Facile colorimetric detection of Hg 2+ based on anti-aggregation of silver nanoparticles. *Biosens. Bioelectron.* 2014, 57, 139–142.
[202] Bhatt KD, Vyas DJ, Makwana BA, Darjee SM, Jain VK. Highly stable water dispersible calix [4] pyrrole octa-hydrazide protected gold nanoparticles as colorimetric and fluorometric chemosensors for selective signaling of Co (II) ions. *Spectrochim. Acta A* 2014, 121, 94–100.
[203] Hao J, Xiong B, Cheng X, He Y, Yeung ES. High-throughput sulfide sensing with colorimetric analysis of single Au-Ag core-shell nanoparticles. *Anal. Chem.* 2014, 86, 4663–4667.
[204] Li W, Qiang W, Li J, Li H, Dong Y, Zhao Y, Xu D. Nanoparticle-catalyzed reductive bleaching for fabricating turn-off and enzyme-free amplified colorimetric bioassays. *Biosens. Bioelectron.* 2014, 51, 219–224.
[205] Kumar VV, Anbarasan S, Christena LR, SaiSubramanian N, Anthony SP. Bio-functionalized silver nanoparticles for selective colorimetric sensing of toxic metal ions and antimicrobial studies. *Spectrochim. Acta A* 2014, 129, 35–42.
[206] Alizadeh A, Khodaei MM, Hamidi Z, Bin Shamsuddin M. Naked-eye colorimetric detection of Cu 2+ and Ag+ ions based on close-packed aggregation of pyridines-functionalized gold nanoparticles. *Sensor. Actuator. B* 2014, 190, 782–791.
[207] Mudabuka B, Ondigo D, Degni S, Vilakazi S, Torto N. A colorimetric probe for ascorbic acid based on copper-gold nanoparticles in electrospun nylon. *Microchim. Acta.* 2014, 181, 395–401.
[208] Pramanik S, Pingguan-Murphy B, Osman NA. Developments of immobilized surface modified piezoelectric crystal biosensors for advanced applications. *Int. J. Electrochem. Sci.* 2013, 8, 8863–8892.
[209] Heydari S, Haghayegh GH. Application of nanoparticles in quartz crystal microbalance biosensors. *Journal of Sensor Technology.* 2014, 2014.
[210] Guo X, Lin C-S, Chen S-H, Ye R, Wu VC. A piezoelectric immunosensor for specific capture and enrichment of viable pathogens by quartz crystal microbalance sensor, followed by detection with antibody-functionalized gold nanoparticles. *Biosens. Bioelectron.* 2012, 38, 177–183.
[211] Xie Y, Jin Y, Huang Y, Liu G, Zhao R. Highly selective piezoelectric sensor for lead (II) based on the lead-catalyzed release of gold nanoparticles from a self-assembled nanosurface. *Microchim. Acta.* 2014, 181, 1521–1527.
[212] Brolo AG. Plasmonics for future biosensors. *Nat. Photon.* 2012, 6, 709–713.
[213] Kojima R, Aubel D, Fussenegger M. Novel theranostic agents for next-generation personalized medicine: small molecules, nanoparticles, and engineered mammalian cells. *Curr. Opin. Chem. Biol.* 2015, 28, 29–38.
[214] Sadik OA, Wanekaya AK, Andreescu S. Advances in analytical technologies for environmental protection and public safety. *J. Environ. Monit.* 2004, 6, 513–522.
[215] Sabelnikov A, Zhukov V, Kempf R. Probability of real-time detection versus probability of infection for aerosolized biowarfare agents: a model study. *Biosens. Bioelectron.* 2006, 21, 2070–2077.
[216] Spindel S, Sapsford KE. Evaluation of optical detection platforms for multiplexed detection of proteins and the need for point-of-care biosensors for clinical use. *Sensors (Basel).* 2014, 14, 22313–22341.
[217] Ghafar-Zadeh E. Wireless integrated biosensors for point-of-care diagnostic applications. *Sensors (Basel).* 2015, 15, 3236–3261.
[218] Srinivasan B, Tung S. Development and applications of portable biosensors. *J. Lab. Autom.* 2015, 20, 365–389.
[219] Zhang D, Liu Q. Biosensors and bioelectronics on smartphone for portable biochemical detection. *Biosens. Bioelectron.* 2016, 75, 273–284.

Bionotes

Hedieh Malekzad
Faculty of Chemistry, Kharazmi University, South Mofatteh Ave, P.O. Box 15719-14911, Tehran, Iran; and Advanced Nanobiotechnology and Nanomedicine Research Group (ANNRG), Iran University of Medical Sciences, Tehran, Iran

Hedieh Malekzad obtained her BSc degree in pure chemistry from the University of Tabriz in 2009. Then, she received her MSc degree in analytical chemistry in 2012 from Kharazmi University, Tehran, Iran. Her research areas and interests encompass analytical techniques for antidoping purposes, computational chemistry, and in particular developing electrochemical metal NP-based biosensors. In 2015, she joined ANNRG to collaborate in professor Karimi's research center, studying various applications of nanoparticles in nanomedicine, including biosensing and biodetection, drug delivery systems, etc.

Parham Sahandi Zangabad
Advanced Nanobiotechnology and Nanomedicine Research Group (ANNRG), Iran University of Medical Sciences, Tehran, Iran; Research Center for Pharmaceutical Nanotechnology (RCPN), Tabriz University of Medical Science (TUOMS), Tabriz, Iran; Department of Materials Science and Engineering, Sharif University of Technology, P.O. Box 11365-9466, 14588 Tehran, Iran

Parham Sahandi Zangabad graduated with a BSc degree from Sahand University of Technology (SUT), Tabriz, Iran, in 2011. In 2014, he received his MSc in nanomaterials/nanotechnology from Sharif University of Technology (SUT), Tehran, Iran. There, he was a research assistant at the Research Center for Nanostructured and Advanced Materials, SUT, Tehran, Iran. During his BSc and MSc research, he worked on the assessment of microstructural/mechanical properties of friction stir-welded nanocomposites. Furthermore, he has carried out research on the synthesis and characterization of sol-gel fabricated ceramic nanocomposite particles. His research covers innovative nanomaterials and nanotechnology in interfacial sciences/technologies and also nanomedicine, including nanoparticle-based drug delivery systems and nanobiosensors. In 2014, he joined ANNRG to collaborate with Prof. Mahdi Karimi's Research lab (ANNRG) in Iran University of Medical Science, Tehran, Iran, in association with Prof. Michael R. Hamblin from Harvard Medical University, Boston, MA, working on smart microcarriers/nanocarriers applied in therapeutic agent delivery systems employed for diagnosis and therapy of various diseases and disorders such as different cancers and malignancies, inflammations, infections, etc. In February 2016, he also made collaborations with Professor Yadollah Omidi, founding director and head of the Research Center for Pharmaceutical Nanotechnology, Tabriz University of Medical Sciences, working on anticancer drug delivery systems for cancer therapy and diagnosis.

Hamed Mirshekari
Advanced Nanobiotechnology and Nanomedicine Research Group (ANNRG), Iran University of Medical Sciences, Tehran, Iran

Hamed Mirshekari received his undergraduate degree in the field of medical laboratory science from Kerman University of Medical Sciences in Iran in 2008. After 2 years working in a hematology laboratory in Tehran, in 2010, he joined to the Biotechnology Department of Kerala University in India and finished his postgraduate project on neural stem cells in the Ragiv Gandhi Center for Biotechnology. Then, in 2014, he joined as research assistant to the Advanced Nanobiotechnology & Nanomedicine Research Group (ANNRG) in Iran University of Medical Sciences in Tehran, Iran, in collaboration with Prof. Hamblin from Harvard Medical School, Boston, MA, USA.

Mahdi Karimi
Department of Medical Nanotechnology, Faculty of Advanced Technologies in Medicine, Iran University of Medical Sciences, Hemmat Exp. Way, P.O. Box 14665-354, Tehran, Iran,
m_karimy2006@yahoo.com, karimi.m@iums.ac.ir

Mahdi Karimi received his BSc degree in medical laboratory science from the Iran University of Medical Science (IUMS) in 2005. In 2008, he received his MSc degree in medical biotechnology from Tabriz University of Medical Science and joined the Tarbiat Modares University as a PhD student in the nanobiotechnology field and completed his research in 2013. During his research, in 2012, he became affiliated with the laboratory of Prof Michael Hamblin in the Wellman Center for Photomedicine at Massachusetts General Hospital and Harvard Medical School as a visiting researcher, where he contributed to the design and construction of new smart NPs for drug/gene delivery. After finishing this study, in 2013, he joined the Department of Medical Nanotechnology at IUMS as an assistant professor, and there, he established a research group named "Advanced Nanobiotechnology and Nanomedicine Research Group" (ANNRG), studying and working on smart drug delivery systems and other nanomedical applications of nanoparticles. His current research interests include design of smart NPs for drug/gene delivery, nanobiosensors, and microfluidic systems. He has established a scientific collaboration between his lab and Prof. Michael Hamblin's lab to design new classes of smart nanovehicles as drug/gene delivery systems.

Michael R. Hamblin
Wellman Center for Photomedicine, Massachusetts General Hospital, Boston, MA 02114, USA; Department of Dermatology, Harvard Medical School, Boston, MA 02115, USA; and Division of Health Sciences and Technology, Harvard-MIT, Cambridge, MA 02139, USA
hamblin@helix.mgh.harvard.edu

Michael R. Hamblin is a principal investigator at the Wellman Center for Photomedicine at Massachusetts General Hospital, is an associate professor of dermatology at Harvard Medical School, and is a member of the affiliated faculty of the Harvard-MIT Division of Health Science and Technology. He was trained as a synthetic organic chemist and received his PhD from Trent University in England. His research interests lie in the areas of photodynamic therapy (PDT) for infections, cancer, and stimulation of the immune system and in low-level light therapy for wound healing, arthritis, traumatic brain injury, neurodegenerative diseases, and psychiatric disorders. He directs a laboratory of around a dozen postdoctoral fellows, visiting scientists and graduate students. His research program is supported by NIH, CDMRP, USAFOSR, and CIMIT, among other funding agencies. He has published over 340 peer-reviewed articles and over 150 conference proceedings, book chapters, and international abstracts and holds eight patents. He has an h-index of 75 and his work has been cited over 20,000 times. He is associate editor for eight journals, is on the editorial board of a further 20 journals, and serves on NIH Study Sections. For the past 11 years, Professor Hamblin has chaired an annual conference at SPIE Photonics West entitled "Mechanisms for Low Level Light Therapy" and he has edited the 11 proceeding volumes together with seven other major textbooks on PDT and photomedicine. He has several other book projects in progress at various stages of completion. In 2011, Dr. Hamblin was honored by election as a Fellow of SPIE. He is a visiting professor at universities in China, South Africa, and Northern Ireland.